borders could not be distinguished, were not included for the counting. From the average grain number per cell of the section labeled with the antisense probe for C1q A mRNA, the average background grain number per cell of the subjacent section labeled with the sense probe for C1q A mRNA was subtracted to get the net grain number per cell. Data were expressed as mean number (±SEM) of grains per C1q A mRNA-positive cell per experimental group.

Quantification of cells immunopositive for C1q and/or the proliferation marker Ki67

Three to eight interval sections per area and per monkey with double IHC for C1q and Ki67 were analyzed at a magnification which allowed the discrimination of cellular features. Immunopositive cells with a nucleus were counted in more than four random 0.1 mm^2 areas per section of insular, occipital, and basofrontal cortices, striatum, and corpus callosum. Dark blue cell nuclei stained for Ki67 and cells stained brown for C1q were counted. Then, the cells co-stained for C1q and Ki67 were counted. In animals exhibiting AIDS (SIV,+AIDS and SIV,+AIDS,+ddG), the number of C1q- and/or Ki67-positive cells, which were parenchymal, intravascular, and perivascular, were counted separately. For total number of cells, all three were summed. Each multinucleated giant cell and cluster of cells, where the individual cell borders could not be distinguished, were counted as single cells having one nucleus. Quantitative image analysis was performed with the MCID M4 image analysis system (Imaging Research, St. Catharines, ON, Canada). Data were expressed as mean number (±SEM) of cell per 0.1 mm^2 area per experimental group.

Statistics

One-way non-parametric analysis of variance (ANOVA) and the post hoc Newman–Keuls Multiple Comparison Test were used to evaluate statistical differences between the experimental groups. Unpaired, two-tailed Student's t test was assessed when comparing antiretroviral untreated and treated AIDS-diseased animal groups. Values of P less than 0.05 were considered statistically significant.

Results

Brain tissue sections of non-infected control monkeys (Ctrl), SIV-infected monkeys without AIDS (SIV,−AIDS), and SIV-infected monkeys exhibiting AIDS (SIV,+AIDS) were analyzed. A fourth group consisted of monkeys with high viremia and increased viral load in CSF at initiation of antiretroviral treatment and suffering from AIDS (SIV,+AIDS,+ddG). All animals are summarized in Table 1.

Table 1
Infection duration, treatment regime, brain virus burden, and signs of encephalitis in monkeys at time of euthanasia and necropsy

Monkey number	Duration of infection (months)	Drug treatment	Brain SIV burden[c]	Degree of SIV-induced encephalitis[d]	Clinical findings
44	Not infected	Not treated	−	−	No disease
50	Not infected	Not treated	−	−	No disease
69	Not infected	Not treated	−	−	No disease
87	Not infected	Not treated	−	−	No disease
75	2.5	Not treated	−	−	Asymptomatic
80	6.5	Not treated	−	−	Asymptomatic
85	4.5	Not treated	−	−	Asymptomatic
92	6.0	Not treated	−	−	Asymptomatic
93	4.5	Not treated	−	−	Asymptomatic
46	19.0	Not treated	+	+	Diarrhea, mycotic infection, mass
71	6.5	Not treated	++	++	Diarrhea, listless, rash
74	6.0	Not treated	+++	+++	Diarrhea, anemia, parasitic infection, LN atrophy
78	2.4	Not treated	+++	+++	Diarrhea, parasitic infection, pneumonitis
79	2.5	Not treated	+	+	Rash, heart murmur, LN atrophy
82	3.0	Not treated	+++	+++	Diarrhea, wasting
86	4.5	Not treated	+++	+++	Wasting, mass, thrush, colitis, LN atrophy
90	2.3	Not treated	++	++	Vomiting, wasting, tube feed
76[a]	22.0	ddI/6-Cl-ddG	−	−	Wasting, diarrhea, heart murmur, anemia
77[a]	4.0	ddI/6-Cl-ddG	±	±	Incontinence, washing, diarrhea
89[b]	22.0	6-Cl-ddG	−	−	Anemia, wasting, diarrhea, lymphoma
91[a]	6.1	ddI/6-Cl-ddG	−	−	Wasting, diarrhea

6-Cl-ddG, 6-chloro-2′,3′-dideoxyguanosine; ddI, 2′,3′-diodeoxyinosine; LN, lymph node; SIV, simian immunodeficiency virus.

[a] Treatment with ddI prior with the CNS-permeant 6-Cl-ddG.

[b] Treatment only with 6-Cl-ddG.

[c] Detection of SIV *env/pol* by ISH; detection of SIV *gp41* by IHC. Scoring: −(ISH: no cells with more silver grains above background, defined as signal with the sense control probes and IHC: no immunoreactive cells) to +++ (ISH: >100 cells/mm^2 with intense collections of silver grains and IHC: >100 immunoreactive cells/mm^2); the numbers of cells/mm^2 were not specifically determined; sections from frontal, insular and occipital cortex, hippocampus, basal ganglia, thalamus, and brainstem were analyzed and summarized.

[d] SIV-induced mononuclear reactions monitored by IHC for RCA-120 or CD-68; scoring was as: +++ for severe, ++ for moderate, and + for mild SIV-induced encephalitis with appearance of macrophage nodules, mononuclear cell infiltrates, multinucleated giant cells, − for non-SIV-induced encephalitis.

Brain C1q protein and mRNA levels in early and late stage of SIV infection

Biosynthesis and regulation of C1q was examined at the transcriptional and translational level in the monkey central nervous system during SIV infection. IHC and ISH for C1q protein and mRNAs encoding the C1q peptide chains A, B, and C were carried out on brain tissue sections of non-infected control monkeys (Ctrl), SIV-infected monkeys without clinical symptoms of AIDS (SIV,−AIDS), and infected monkeys exhibiting AIDS (SIV,+AIDS). Immunohistochemistry for C1q revealed only few immunoreactive cells in cortical gray and white matter of non-infected monkeys as demonstrated for the insular cortex (Fig. 1A). SIV infection caused a moderate increase in the number of C1q-immunopositive cells and in the intensity of C1q cell immunoreactivity in insular cortex in early unproductive stage of disease (Fig. 1B). An even stronger increase in the number of C1q-immunostained cells was observed in late stage of disease with clinical manifestation of AIDS (Fig. 1C). Next, we explored whether the three C1q chains A, B, and C were co-upregulated, as

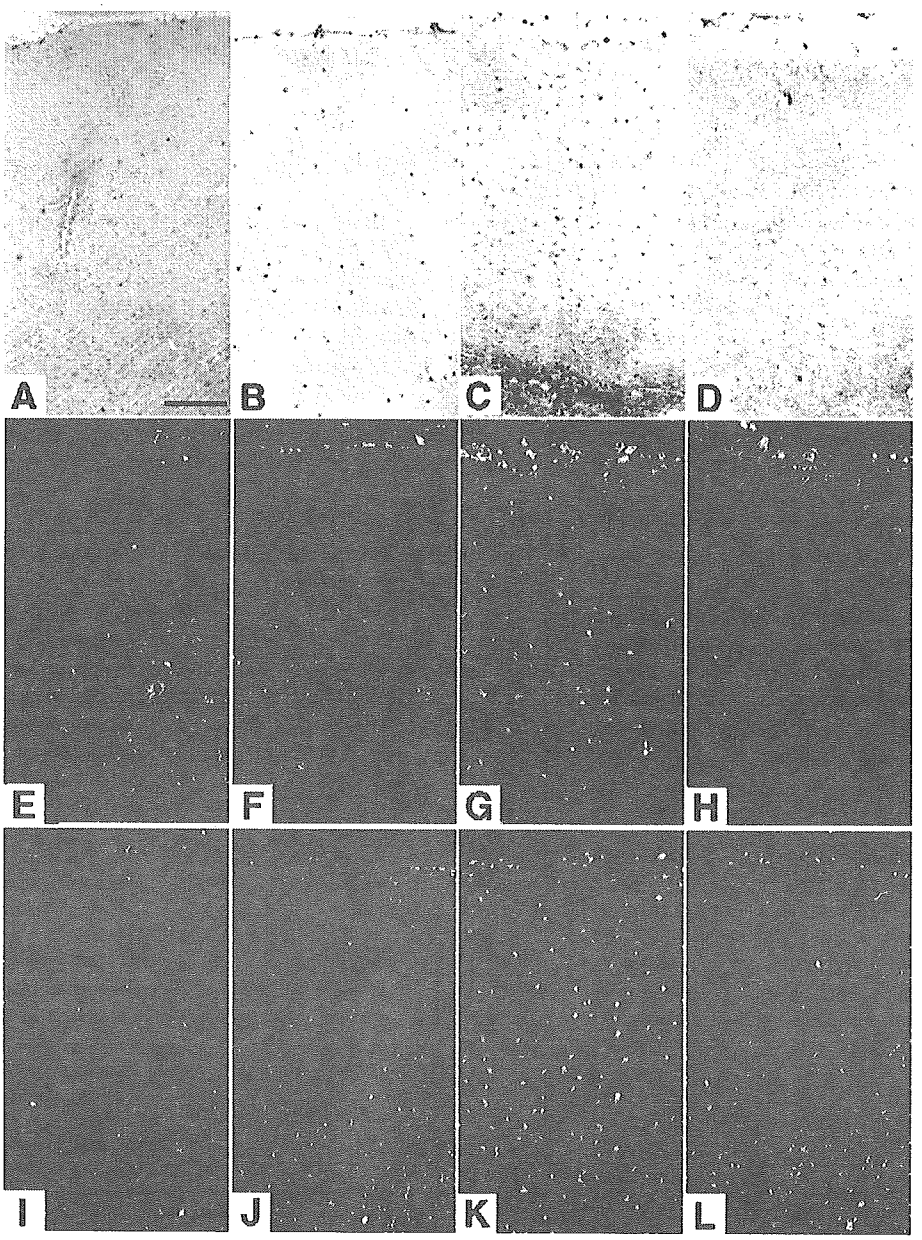

Fig. 1. Regulation of C1q protein and mRNA encoding C1q A and B chains in the rhesus monkey insular cortex in control (A, E and I), SIV infection without AIDS (B, F and J), SIV infection with AIDS (C, G and K) and SIV infection with AIDS and antiretroviral treatment (D, H and L). C1q-immunoreactivity is moderately increased in the insular cortex of monkeys without AIDS (B) and more strongly increased in monkeys exhibiting AIDS (C) as compared to non-infected control monkeys (A). After antiretroviral treatment of monkeys exhibiting AIDS, the number of C1q-immunoreactive cells is similar to that in early stages of disease (D). In situ hybridization signals for mRNA of C1q chains A and B are abundant in the insular cortex of monkeys with AIDS (G and K) as compared to control (E and I). After antiretroviral treatment, the number of cells demonstrating signals for C1q A and B mRNA (H and L) is similar to levels in the SIV,-AIDS group (F and J). Scale bar in A for A–L is 200 μm.

biologically active C1q protein requires the co-expression of all three C1q chains. The antibody we employed did not differentiate between the three C1q peptide chains; therefore, in situ hybridization was carried out to localize the three C1q transcripts.

In situ hybridization with [^{35}S]-labeled cRNA antisense probes demonstrated a similar pattern of changes in C1q A, B, C mRNA expression throughout all telencephalic lobes, hippocampus, striatum, and brainstem nuclei, indicating that bioactive C1q was produced. The changes of C1q mRNA expression in the four experimental groups are demonstrated for the C1q A and B chains (Figs. 1E–G and 1I–K). A marked increase in the density of cells expressing C1q A and B mRNAs was observed in the insular cortex of monkeys with AIDS. C1q mRNA was found to be copious in the cortex of SIV,+AIDS monkeys, and was distributed in a uniform, non-laminar pattern suggesting a non-neuronal localization. SIV-infected monkeys without AIDS exhibited only a moderate increase in cells expressing C1q mRNAs which occurred mainly in submeningeal spaces.

To quantify the observed changes of C1q mRNA and protein expression during SIV infection, cells stained for the C1q A chain mRNA shown to be representative for the B and C chains and C1q protein were counted. A dramatic increase in the number of cells expressing C1q A mRNA in the striatum and the insular cortex of monkeys with AIDS (43.9 ± 10.0 and 38.5 ± 7.5 cells per 0.1 mm^2 area) was observed (Table 2) as compared to the animals of the control (0.5 ± 0.1 and 0.4 ± 0.1 cells per 0.1 mm^2 area) or SIV,−AIDS groups (0.6 ± 0.4 and 0.5 ± 0.1 cells per 0.1 mm^2 area). Counting of C1q-immunopositive cells revealed an early upregulation of C1q protein biosynthesis during SIV infection before clinical symptoms became apparent (Table 2). In striatum and insular cortex of SIV,−AIDS animals, 7.9 ± 1.9 and 6.8 ± 3.7 cells per 0.1 mm^2 area, respectively, were detected as compared to control striatum and insular cortex (1.0 ± 0.2 and 2.3 ± 2.2 cells per 0.1 mm^2 area, respectively). In AIDS-diseased animals, even more C1q-immunoreactive cells were seen in the striatum (44.4 ± 7.5 cells per 0.1 mm^2 area) and in the insular cortex (40.6 ± 5.8 cells per 0.1 mm^2 area). Table 3 demonstrates additionally the number of C1q-immunopositive cells per area in occipital cortex, basofrontal cortex, and in corpus callosum of the Ctrl, SIV,−AIDS, and SIV,+AIDS groups. Grain counting revealed a significant ($P < 0.05$) increase in the C1q A mRNA abundance per cell in the brain of monkeys with AIDS as compared to non-infected monkeys and infected monkeys without AIDS (Table 2).

Table 2
Quantification of C1q protein-positive and C1q A mRNA-positive cells as well as of grains per C1q A mRNA-positive cell in the brain of rhesus macaques during SIV infection and antiretroviral treatment

Monkey groups	Insular cortex	Striatum
C1q protein-positive cells[a]		
Ctrl	2.3 ± 2.2	1.0 ± 0.2
SIV,−AIDS	6.8 ± 3.7	7.9 ± 1.9[c]
SIV,+AIDS	40.6 ± 5.8[b]	44.4 ± 7.5[b]
SIV,+AIDS,+ddG	6.8 ± 2.8	5.2 ± 2.0[c]
C1q A mRNA-positive cells[a]		
Ctrl	0.4 ± 0.1	0.5 ± 0.1
SIV,−AIDS	0.5 ± 0.1	0.6 ± 0.4
SIV,+AIDS	38.5 ± 7.5[b]	43.9 ± 10.0[b]
SIV,+AIDS,+ddG	9.3 ± 2.8[d]	9.2 ± 3.2[d]
Grains per C1q A mRNA-positive cell		
Ctrl	48.5 ± 9.1	41.1 ± 25.4
SIV,−AIDS	64.2 ± 10.7	62.2 ± 16.3
SIV,+AIDS	152.1 ± 22.6[b]	160.4 ± 24.5[b]
SIV,+AIDS,+ddG	82.0 ± 24.3	78.5 ± 24.3

ANOVA and the post hoc Newman–Keuls Multiple Comparison Test are used to evaluate statistical differences.

[a] Data expressed as mean number (±SEM) of C1q-positive cells per 0.1 mm^2 area.

[b] Statistically significantly different as compared to the other animal groups for the same brain area.

[c] Statistically significantly different only as compared to Ctrl group for the same brain area ($P < 0.05$).

[d] Statistically significantly different only as compared to Ctrl and SIV,−AIDS groups for the same brain area ($P < 0.05$).

Antiretroviral treatment and C1q protein and mRNA levels in the brain

To determine the impact of viral burden on the C1q biosynthesis in brain tissue, SIV-infected monkeys with high viremia and increased viral load in CSF were treated with 2′,3′-dideoxyinosine (ddI) for clinical stabilization followed by lipophilic 6-chloro-2′,3′-dideoxyguanosine (6-Cl-ddG). Only one animal (MO89) was treated only with 6-Cl-ddG. All animals receiving antiretroviral treatment with either ddI followed by 6-Cl-ddG or with 6-Cl-ddG alone exhibited clinical symptoms of AIDS (SIV,+AIDS,+ddG). In these four antiretrovirally treated animals, only minor upregulation of C1q was seen (Figs. 1D, H, and L) independently of whether they received combinatorial treatment or treatment with 6-Cl-ddG alone. This justifies analyzing these antiretrovirally treated animals as a group, though not homogeneous. Cell counting in striatum and insular cortex revealed that monkeys of the treated group had a higher density of cells expressing C1q A mRNA (9.2 ± 3.2 and 9.3 ± 2.8 cells per 0.1 mm^2 area, respectively) and C1q protein (5.2 ± 2.0 and 6.8 ± 2.8 cells per 0.1 mm^2 area, respectively) than monkeys of the Ctrl or SIV,−AIDS groups. Table 3 demonstrates additionally the density of C1q-immunopositive cells in occipital cortex, basofrontal cortex, and in corpus callosum of the SIV,+AIDS,+ddG group. As compared to non-treated AIDS-positive animals, all animals receiving antiretroviral treatment had a lower number of cells expressing C1q A mRNA and protein per area in the insular cortex and the striatum. The average grain number per C1q A mRNA-expressing cell was selectively increased in untreated symptomatic animals as compared to the other three groups (Table 2). Thus, antiretroviral treatment seemed to reduce C1q mRNA per cell in animals with AIDS.

Cellular expression of C1q protein and mRNA encoding C1q peptide chains A, B, and C

To identify the cell types producing C1q, high-power confocal laser scanning analysis was carried out after double immunofluorescence for C1q and the well-established microglia/macrophage activity marker CD-68, the astroglial marker GFAP, the oligodendroglial marker CNPase, the endothelial cell marker von Willebrand factor vWF, and the neuronal marker NeuN, respectively. C1q was co-localized with CD-68 in microglia/macrophages and multinucleated giant cells (Figs. 2A, B) but was absent from GFAP-positive astrocytes and CNPase-positive

Table 3
Proportional analysis of C1q-positive cells with Ki67-immunoreactivity in different brain regions during SIV infection and antiretroviral treatment

Monkey groups[a]	Brain regions	$C1q^+$	$Ki67^+$	$C1q^+/Ki67^+$
Ctrl	Insular cortex	2.3 ± 2.2	0.1 ± 0.1	0.1 ± 0.1
	Occipital cortex	4.9 ± 2.6	0	0
	Basofrontal cortex	1.7 ± 1.3	0.1	0.1
	Striatum	1.0 ± 0.2	0.2 ± 0.1	0.1 ± 0.1
	Corpus callosum	1.2 ± 0.2	0.7 ± 0.5	0.4 ± 0.3
SIV,−AIDS	Insular cortex	6.8 ± 3.7	0.9 ± 0.8	0.9 ± 0.7
	Occipital cortex	12.9 ± 3.2[b]	1.4 ± 0.7	1.3 ± 0.8
	Basofrontal cortex	10.0 ± 5.5[b]	1.3 ± 0.6	1.2 ± 0.6
	Striatum	7.9 ± 1.9[b]	1.6 ± 0.8	1.6 ± 0.7
	Corpus callosum	8.8 ± 1.6[b]	6.0 ± 3.1[b]	5.3 ± 2.5[b]
SIV,+AIDS	Insular cortex	40.6 ± 5.6[c]	14.0 ± 7.0[d]	12.7 ± 6.3[c]
	Occipital cortex	48.3 ± 9.4[c]	7.3 ± 4.1[d]	6.9 ± 4.0[c]
	Basofrontal cortex	40.3 ± 6.9[c]	8.6 ± 3.7[d]	8.1 ± 3.4[c]
	Striatum	44.4 ± 7.5[c]	17.8 ± 7.0[d]	16.5 ± 7.0[d]
	Corpus callosum	38.6 ± 11.6[c]	18.4 ± 4.8[c]	17.6 ± 5.6[d]
SIV,+AIDS,+ddG	Insular cortex	6.8 ± 2.8	8.1 ± 5.1[d]	2.4 ± 1.1[b]
	Occipital cortex	9.1 ± 4.3	7.3 ± 3.6[d]	3.5 ± 1.7[b]
	Basofrontal cortex	8.2 ± 3.2[b]	7.3 ± 2.1[d]	3.7 ± 1.2[b]
	Striatum	5.2 ± 2.0[b]	8.8 ± 4.9[d]	2.7 ± 1.3[b]
	Corpus callosum	5.2 ± 2.1[b]	6.8 ± 3.1[b]	2.7 ± 0.7[b]

ANOVA and the post hoc Newman–Keuls Multiple Comparison Test are used to evaluate statistical differences.
[a] Data expressed as mean number (±SEM) of C1q-, Ki67-positive, or C1q-/Ki67-co-positive cells per 0.1 mm^2 area.
[b] Statistically significantly different only as compared to Ctrl group for the same brain area ($P < 0.05$).
[c] Statistically significantly different as compared to the other animal groups for the same brain area ($P < 0.05$).
[d] Statistically significantly different only as compared to Ctrl and SIV,−AIDS groups for the same brain area ($P < 0.05$).

oligodendocytes (Figs. 2C, D). C1q protein was not seen in the cytoplasm of neuronal perikarya and was undetectable in endothelial cells (Figs. 2E, F).

Additionally, co-localization experiments were performed by combining IHC and ISH. C1q A mRNA hybridization signals were found in isolectin-positive microglia, macrophages, and multi-

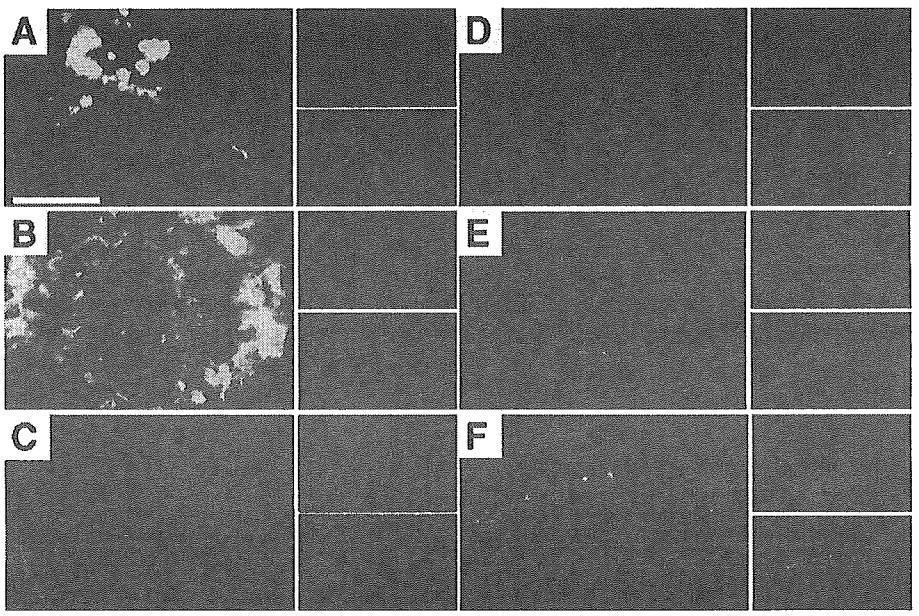

Fig. 2. Identification of C1q-positive cell types. Confocal laser scanning images of double immunofluorescence demonstrating co-existence of C1q (red) with the activation marker CD-68 (green) in a single microglia/macrophage and in a multinucleated giant cell (A and B) and segregation of C1q (red) with the established markers of brain resident cells (green)-glial fibrillary acid protein (GFAP) for astrocytes (C), 2′,3′-cyclic nucleotide-3′-phosphodiesterase (CNPase) for oligodendrocytes (D), neuronal antigen NeuN for neurons (E), and van Willebrand factor (vWF) for endothelial cells (F). A minimum of about 500 cells were examined for each cell type for each SIV-infected animal with AIDS (SIV,+AIDS) to make definitive statements. Scale bar in A for A–F is 10 μm in single-colored micrographs and 5 μm in micrographs with overlayed colors.

nucleated giant cells (Figs. 3A, B) in brains of monkeys with AIDS, but were totally absent from isolectin-positive endothelial cells (Figs. 3A, B). C1q protein was co-localized with its mRNA as shown for subependymal macrophages and macrophages adherent on the ependymal surface (Fig. 3C, D). Double ISH revealed the presence of transcripts encoding all three chains of C1q in diffusely distributed as well as in nodule and syncytium forming microglia/macrophages (Figs. 4A, B) and confirmed the absence of C1q biosynthesis in endothelial cells and neuronal cell bodies (Fig. 4C). Ependymal cells neither exhibited hybridization signals for C1q mRNA nor were they C1q-immunoreactive. In all animal groups, C1q A, B, and C mRNAs were not detected in neurons. However, in the absence of neuronal synthesis of C1q, a variable number of neurons throughout the brain exhibited deposition of immunopositive C1q on the surface membrane of their somata and processes (Figs. 5A, B), both in control and in infected animals, with no obvious difference between the four experimental groups.

Relationship of C1q expression to cell proliferation and influence of antiretroviral treatment

To determine whether the level of C1q expression is due to SIV-induced cell proliferation, double IHC for C1q and the nuclear proliferation marker Ki67 was carried out. Ki67-immunostaining revealed very few proliferating cells which were mainly found in perivascular areas, both in the brains of control and asymptomatically infected animals. The clinical manifestation of disease was characterized by an increase of proliferation in perivascular areas and an appearance of proliferating cells adhering to the luminal endothelium as well as by an induction of diffuse cell proliferation in the brain parenchyma (Fig. 6). To determine the correlation between C1q-positive cells and Ki67-positive proliferating cells, computer-assisted comparative cell counting was performed as demonstrated for the insular, occipital, and basofrontal cortices, for the striatum and for the corpus callosum (Table 3). In monkey brains of the SIV,+AIDS group, 92–97% of proliferating cells were C1q-immunoreactive. In antiretrovirally treated animals, the number of cells labeled for C1q alone or co-labeled for C1q and Ki67 was similar to that in infected animals without AIDS. Antiretroviral treatment had no significant influence on the total number of Ki67-positive cells as compared to untreated AIDS-diseased animals except for the corpus callosum (Figs. 6A–D; Table 3). However, parenchymal accumulation of Ki67-positive proliferating cells seen in untreated animals was absent in all four animals receiving antiretroviral treatment. In contrast, the vessel-associated cell proliferation seen in the SIV,+AIDS group was largely unaffected by the antiretroviral treatment (Table 4). The different proliferating or non-proliferating C1q-positive cell types observed in the brain of monkeys with AIDS were assessed by double IHC for C1q and Ki67 (Fig. 7).

Adherence of C1q-positive cells on the endothelium in late stage of SIV infection and influence of antiretroviral treatment

Adherence of inflammatory cells on the luminal endothelium is regarded as a morphological sign for infiltration of cells through the blood–brain barrier (Williams and Hickey, 1995). Our quantitative analysis revealed an increase in the number of C1q-immunostained cells adhering on the luminal side of the endothelium in the brain of monkeys with AIDS ($P < 0.05$), especially in areas with accumulation of macrophages and multinucleated giant cells known as hallmarks of productive SIV infection. Apparently, these cells were truly adherent and in the progress of infiltrating into the brain as they were not washed away by the transcardial perfusion prior to or during fixation procedures. Antiretroviral treatment was found to reduce the number of C1q-positive cells attached to the endothelium (Table 5).

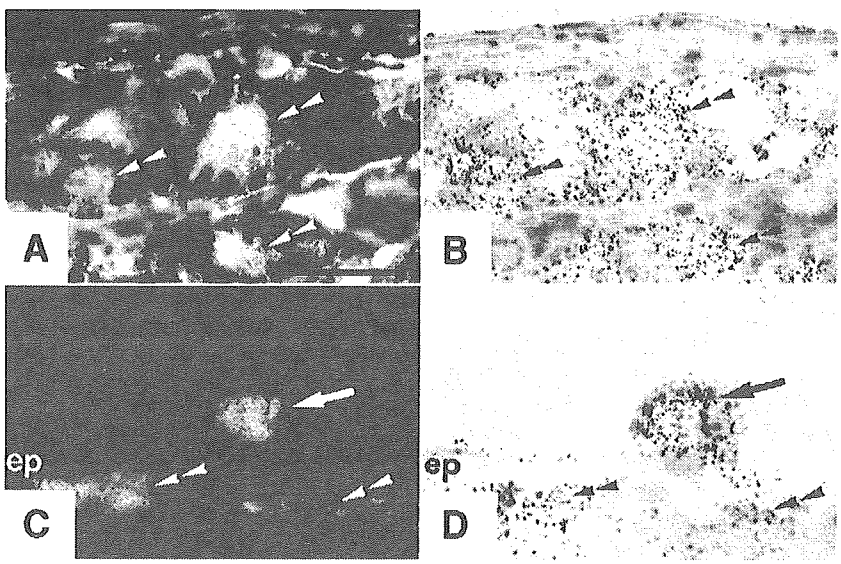

Fig. 3. Combinatorial in situ hybridization and immunofluorescence on identical brain sections of an untreated monkey with AIDS. (A and B) Hybridization signals for C1q A mRNA are present in isolectin-positive macrophages and multinucleated giant cells (double arrowheads) but not in isolectin-positive endothelial cells. (C and D) In situ hybridization signals for C1q A mRNA in C1q-immunopositive cells adherent on the ependymal surface (arrows) and lying subependymally (double arrowheads). Note the absence of C1q expression from ependymal cells (ep), which are negative for both C1q protein and C1q mRNA. Scale bar in A for A–D is 10 μm.

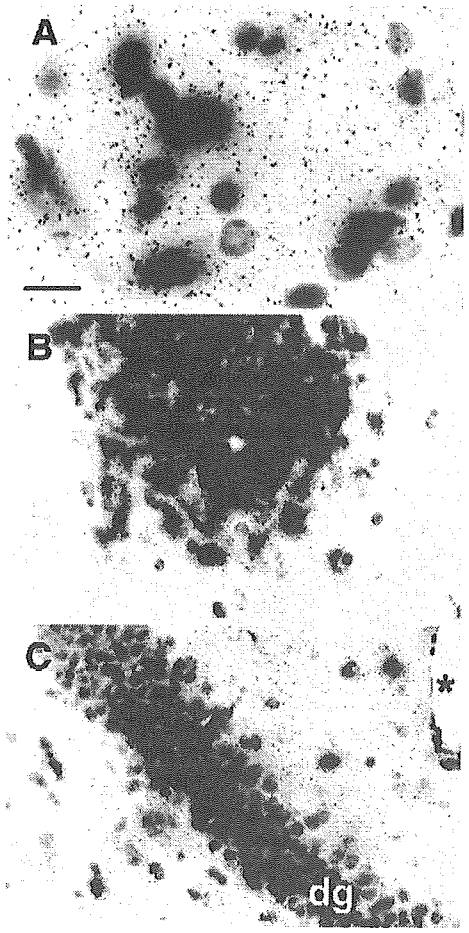

Fig. 4. Co-hybridization for mRNA encoding C1q peptide chains A, B, and C in the brain of monkeys with AIDS. (A) Transcript for C1q chains B (dark blue reaction) and C (silver grains) in diffusely distributed microglia/macrophages. (B and C) Message for C1q chains A (blue reaction) and C (silver grains) is present in nodule and giant cell forming as well as in diffusely distributed macrophages. Note the absence of transcripts of C1q A and C1q C chains from dentate gyrus (dg) neurons and endothelia of a blood vessel (asterisk). Scale bar in A for A–C is 50 μm.

Brain viral burden and CNS-selective antiretroviral treatment

The effect of antiretroviral treatment on brain viral burden is summarized in Table 1. There was little evidence that the SIV replicated in the CNS in the asymptomatic stage of infection. SIV RNA- and SIV glycoprotein *gp41*-positive cells were mainly detected in the animals with clinical symptoms of AIDS and with SIV encephalitis. Only cells of the microglia/macrophage-lineage were found to contain SIV RNA and *gp41* protein. There was no evidence for the presence of SIV RNA or SIV gp41 immunoreactivity in astrocytes or endothelial cells under our different experimental conditions. Co-staining experiments for *gp41* and C1q revealed that nearly all C1q-positive multinucleated giant cells were also stained for virus *gp41* (>95%). Most C1q-positive macrophages were *gp41*-positive (70–80%). The microglia compartment had the lowest number of cells double labeled for C1q and *gp41* (<10%; Fig. 8). Antiviral treatment markedly reduced the number of SIV RNA- and *gp41*-positive cells. The effects of antiviral treatment on viral burden and RCA-120- or CD-68-stained mononuclear reactions in the brain are summarized in Table 1.

Discussion

This study describes the plasticity of C1q expression in the brain of rhesus monkeys during the course of simian immunodeficiency virus infection. A striking feature is that C1q was globally upregulated in early asymptomatic stage of SIV disease. This early phase of C1q increase was followed by an enhanced C1q expression when clinical symptoms manifested. The former was an increase in the number of C1q-immunoreactive brain resident cells, the latter was a result of C1q gene transcription as well as of proliferation and infiltration of C1q-positive cells in the brain. The susceptibility to antiretroviral treatment with the lipophilic 6-chloro-2′,3′-dideoxyguanosine demonstrated that brain C1q synthesis was directly related to brain SIV burden.

In our study, using IHC and ISH and combination of both techniques, we identified exclusively cells of the mononuclear lineage–microglia, macrophages, and multinucleated giant cells–as the sources of cerebral C1q biosynthesis. Similar observations have been previously reported in the Borna-infected rat brain (Dietzschold et al., 1995). By demonstrating that C1q protein and the three mRNAs encoding the three C1q chains were co-regulated, we provide evidence that functionally intact C1q is synthesized in the brain during SIV infection. Before manifestation of clinical AIDS, virus burden and signs of productive inflammation in the brain were low, and C1q was predominantly found in microglia. In contrast, the late stage was characterized by high viral burden and encephalitis in the brain, and C1q was also found in resident and infiltrating macrophages as well as in multinucleated giant cells.

Antiretroviral treatment of AIDS-diseased monkeys reduced cerebral virus burden and virus-induced encephalitis which resulted in substantial decline of C1q expression in the brain as compared to AIDS-diseased animals receiving no antiretroviral treatment. As the animal receiving 6-Cl-ddG alone (MO89) was effectively treated with respect to reduction of brain virus burden and the degree of SIV-induced encephalitis, we conclude that 6-Cl-ddG is effective independent of pretreatment with ddI.

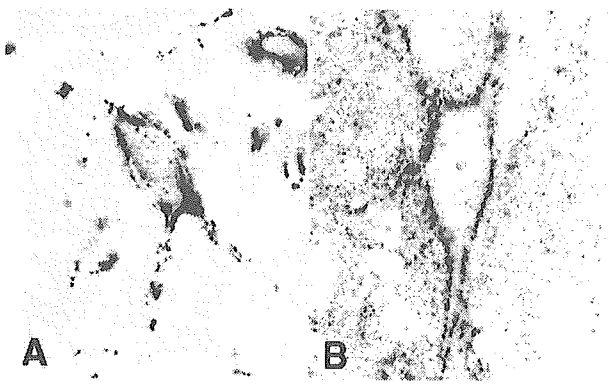

Fig. 5. High-power micrographs demonstrating neuronal surface staining of C1q as shown for a neuron of the substantia nigra pars compacta (A) and a motoneuron of the thoracic spinal cord (B) of a control monkey. Note that the cytoplasm of the perikarya and processes is free from C1q. All monkey brains of all experimental groups demonstrated same staining pattern without obvious difference.

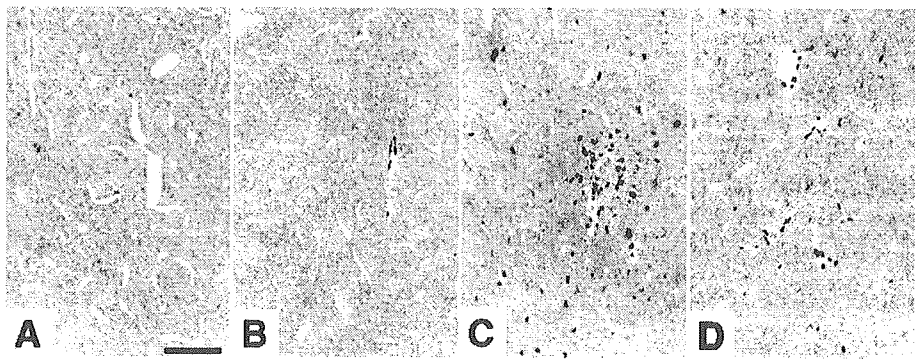

Fig. 6. Effect of antiviral treatment with 6-Cl-ddG on nuclear proliferation antigen Ki67 in the monkey insular cortex. Note the low number of Ki67-stained cell nuclei in the Ctrl and SIV,−AIDS groups (A and B) but high levels in the AIDS-diseased animal groups (C and D). Untreated symptomatic monkeys demonstrate a more diffuse and nodular Ki67 staining (C) in contrast to antiretrovirally treated monkeys exhibiting AIDS which exhibit mainly a vasculature-associated staining for Ki67 (D). Scale bar in A for A–D is 100 μm.

Apparently, the degree of increase in C1q expression correlates with the viral load in the brain. The key observation to be derived from the CNS-permeant and systemic antiretroviral therapy is the tight linkage between brain virus burden and C1q expression in the microglial/macrophage cellular compartment, both positively in late-stage (untreated) AIDS, and negatively in late-stage AIDS accompanied by CNS-permeant plus systemic antiretroviral therapy. Noteworthy, the C1q increase in microglia during clinical latency suggests that microglial activation and neuroinflammatory damage in the brain occur early during SIV infection perhaps through the early presence of SIV in the CNS, although SIV is not replicating in this stage. The effect of 6-Cl-ddG appeared to be cell-specific. It was shown to reduce SIV-induced upregulation of C1q expression in microglial cells and to completely abolish the appearance of C1q expressing macrophages and multinucleated giant cells. Thus, signs of productive inflammation (Budka, 1986; Dickson, 1986; Kato et al., 1987; Lane et al., 1996; Lifson et al., 1986; Williams et al., 2001) and the appearance of SIV RNA- and SIV protein-positive cells were markedly decreased by 6-Cl-ddG. Antiretroviral treatment significantly reduced but did not abolish microglial activation. Interestingly, the antiretroviral treatment selectively reduced SIV-induced proliferation of brain parenchymal cells and down-regulated C1q expression in microglia and parenchymal macrophages. In contrast, juxtavascular proliferation was partly resistant to antiretroviral treatment while an increase of C1q biosynthesis in intravascular and perivascular cells of the monocyte/macrophage-lineage was blocked by the treatment. The dissociated effectiveness of 6-Cl-ddG treatment in CNS tissues and the relative resistance to that treatment in peripheral cells may be explained by the better uptake of the lipophilic 6-Cl-ddG by CNS cells.

The increased local synthesis of C1q in brain resident and invading cells is likely to be important in the complement-mediated opsonization of SIV (Speth et al., 2002) and modulation of phagocytosis by endothelial cells, macrophages, monocytes, and microglia (Bobak et al., 1987). In addition to pro-

Table 4
Effect of antiretroviral treatment on parenchymal and vasculature-associated cell proliferation

Monkey groups[a]	Brain region	Parenchymal	Vasculature associated[b]
SIV,+AIDS	Insular cortex	8.8 ± 2.1	5.2 ± 1.1
	Occipital cortex	4.6 ± 1.5	2.4 ± 0.7
	Striatum	10.3 ± 1.5	7.6 ± 3.0
SIV,+AIDS,+ddG	Insular cortex	2.4 ± 0.5[c]	5.6 ± 1.9
	Occipital cortex	2.0 ± 0.3[c]	5.2 ± 1.4
	Striatum	1.9 ± 0.5[c]	6.9 ± 1.9

Unpaired, two-tailed Student's t test is used to evaluate statistical differences.

[a] Data expressed as mean number (±SEM) of Ki67-positive cell nuclei per 0.1 mm^2 area.

[b] Proliferating cells demonstrating perivascular or intraluminal endothelial adherent staining.

[c] Statistically significantly reduced as compared to the untreated group for the same brain area ($P < 0.05$).

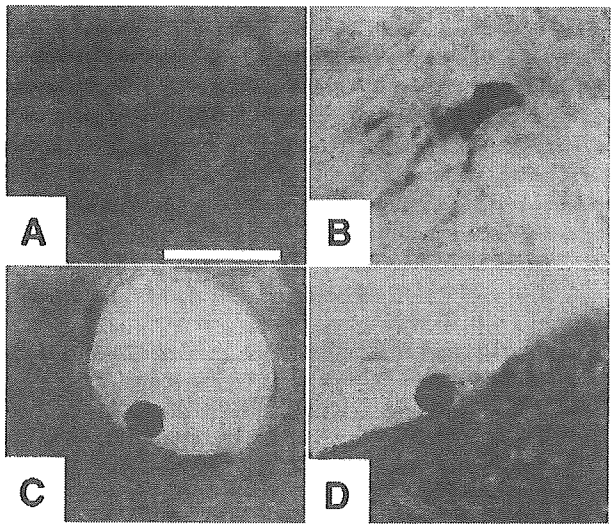

Fig. 7. C1q-positive cells with respect to proliferating and non-proliferating activity in the brain of monkeys with AIDS revealed by double immunohistochemistry for C1q and Ki67. Parenchymal microglia/macrophages (brown, A and B) and vessel-attached monocytes (brown, C and D) demonstrating no Ki67 staining (A and C) or clear nuclear Ki67 staining (nuclear dark blue, B and D). Note that the cell in (B) demonstrates nuclear Ki67 staining typical for a cell undergoing mitosis. Scale bar in A for A–D is 10 μm.

Table 5
Quantitative analysis of C1q-immunopositive cells adhering on the intraluminal surface of cerebrovascular endothelium

Monkey groups[a]	Insular cortex	Occipital cortex	Striatum
Ctrl	0	0	0
SIV,−AIDS	0.3 ± 0.2	0.3 ± 0.2	0.2 ± 0.2
SIV,+AIDS	3.9 ± 1.4[b]	4.6 ± 1.4[b]	4.8 ± 1.6[b]
SIV,+AIDS,+ddG	1.0 ± 0.6	1.2 ± 0.7	0.6 ± 0.3

ANOVA and the post hoc Newman–Keuls Multiple Comparison Test are used to evaluate statistical differences.

[a] Data expressed as mean number (±SEM) of C1q-positive cells per 0.1 mm^2 area.

[b] Statistically significantly different as compared to the other animal groups for the same brain area ($P < 0.05$).

inflammatory effect of C1q on its own, the activation of complement components downstream of C1q may generate soluble mediators which could trigger infiltration of inflammatory cells into the brain directly by chemoattractant properties of complement anaphylatoxins and cleavage products to complement receptor bearing cells (Ghebrehiwet et al., 1995; Kuna et al., 1996; Leigh et al., 1998; Speth et al., 1997) and/or indirectly by upregulation of adhesion molecules like the endothelial P-selectin or chemokines like MCP-1 (Mulligan et al., 1997; van den Berg et al., 1998).

Therefore, we propose that C1q levels in brain are a useful indicator for the severity of inflammatory reactions during lentiviral infections as well as for virus burden. This is of potential significance for monitoring progression and amelioration of SIV-associated neurological disease and for the prognosis of therapeutic interventions by determining C1q levels in the CSF. Changes in CSF levels of mediators of the immune response following antiretroviral therapy in AIDS had been reported previously for immediate early proteins like neopterin and β_2-microglobulin, neurotoxins like quinolinic acid, cytokines and cytokine receptors like MCP-1, TNF-α ligand and its soluble receptor (Conant et al., 1998; Fuchs et al., 1990; Gulevich et al., 1993; Heyes et al., 1989; Look et al., 2000) but not for C1q. Changes of C1q levels in the CSF had been reported in several degenerative and inflammatory neurological diseases and disease models (Antoine et al., 1986; Schäfer et al., 2000; Smyth et al., 1994; Wajgt et al., 1989; Yamada et al., 1994).

There is an ongoing controversy as to whether C1q is expressed in cerebral neurons in the course of neurological disorders, especially in the human brain (Fonseca et al., 2004; Head et al., 2001). Therefore, we paid particular attention to monitoring C1q mRNA and protein expression in neurons throughout the brain in all experimental groups. The total absence of C1q mRNA from neurons and of C1q immunoreactivity from neuronal cytoplasm throughout the brain found in this study provides no evidence that neurons synthesize C1q in normal and diseased rhesus monkey brain. This is in accordance with our previous studies on rodents also showing restriction of C1q expression to microglial/macrophage cells both after CNS virus inflammation and after cerebral ischemia or toxic lesion of the blood–brain barrier (Dietzschold et al., 1995; Lynch et al., 2004; Schäfer et al., 2000).

The deposition of C1q on the outer surfaces seen in the present study in some neurons throughout brains of all experimental groups may be due to deposition of extrinsic C1q most likely coming from local production or from serum through local leakages of the blood–brain barrier. This deposition of C1q on neuronal surfaces may be taken as evidence that a putative C1q receptor is expressed on some neurons (Eggleton et al., 2000; Kishore and Reid, 2000). Our results are in some concordance with immunohistochemical data by Speth et al. (2004) also showing C1q-immunopositive microglial/macrophage cells, but unlike these authors, our study clearly excludes astrocytes and neurons as a source of C1q biosynthesis and provides no evidence that deposition of C1q on neuronal surfaces is causally related to SIV infection.

C1q is one of several response genes of the monocyte/macrophage arm of innate immunity which is regulated during HIV/SIV infection as recently evaluated using DNA array technology in the accelerated CD8-depletion model of SIV-infected rhesus macaques (Roberts et al., 2003). Among them, indoleamine 2,3-dioxygenase is upregulated like C1q in SIV brain disease and is sensitive to antiretroviral treatment (Depboylu et al., 2004). We obtained no evidence for the presence of SIV RNA and protein in astrocytes that certainly exhibit activation during SIV infection as shown previously (Weihe et al., 1993). Astrocytes are likely involved in the retroviral neuropathogenesis, but most evidence does not support widespread infection of them in vivo. For humans, it had been primarily pediatric cases with massive HIV brain infection that had shown infection of astrocytes (Saito et al., 1994; Tornatore et al., 1994). Otherwise, such findings had been observed mainly in vitro/ex vivo, or in models such as the pig-tailed macaque accelerated model characterized by massive CNS infection and very short term disease (Overholser et al., 2003).

In summary, our study provides clear evidence that C1q synthesis is induced in brain resident and infiltrating immune cells following SIV infection and correlates with brain virus load as well as clinical manifestation of simian AIDS. The relationship between C1q expression in microglia/macrophages and multinucleated giant cells, and virus burden may ultimately be useful in revealing the functional association of inflammatory and virological markers during lentiviral infection of the brain, and therefore the role of each in motor/cognitive dysfunction associated with lentiviral infection.

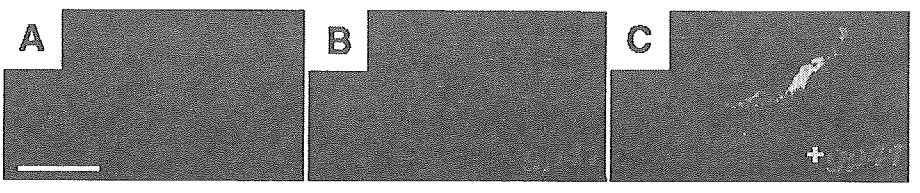

Fig. 8. Double immunofluorescence confocal images demonstrating co-existence of C1q (red) with the SIV glycoprotein *gp41* (green) in a microglia in the brain of an untreated AIDS-diseased animal (A–C). Scale bar in A for A–C is 10 μm.

Acknowledgments

This study was supported by a grant of the Volkswagen Foundation to L. E. Eiden and E. Weihe and the German Research Foundation (Schwerpunkt Mikroglia) to E. Weihe and W. J. Schwaeble. For excellent technical work, we thank R. Vertesi and D. Huddleston from L. E. Eiden's lab as well as E. Rodenberg-Frank, M. Zibuschka, T. Henke, and H. Hlawaty from E. Weihe's lab. For expert photographic assistance, we are indebted to H. Schneider from E. Weihe's lab. Parts of this study were presented at the 31st Annual Meeting of the Society for Neuroscience in San Diego, USA (Depboylu et al., 2001).

References

Antoine, J.C., Michel, D., Lamelin, J.P., Laurent, B., Schott, B., 1986. Cerebrospinal fluid and serum immune complex in acute inflammatory polyneuritis. Detection by C1q binding assay. Acta Neurol. Scand. 73, 477–480.

Bissel, S.J., Wang, G., Ghosh, M., Reinhart, T.A., Capuano III, S., Stefano Cole, K., Murphey-Corb, M., Piatak Jr., M., Lifson, J.D., Wiley, C.A., 2002. Macrophages relate presynaptic and postsynaptic damage in simian immunodeficiency virus encephalitis. Am. J. Pathol. 160, 927–941.

Bobak, D.A., Gaither, T.A., Frank, M.M., Tenner, A.J., 1987. Modulation of FcR function by complement: subcomponent C1q enhances the phagocytosis of IgG-opsonized targets by human monocytes and culture-derived macrophages. J. Immunol. 138, 1150–1156.

Budka, H., 1986. Multinucleated giant cells in the brain: a hallmark of the acquired immunodeficiency syndrome (AIDS). Acta Neuropathol. (Berl.) 69, 253–256.

Conant, K., Garzino-Demo, A., Nath, A., McArthur, J.C., Halliday, W., Power, C., Gallo, R.C., 1998. Major induction of monocyte chemoattractant protein-1 in HIV-1 Tat-stimulated astrocytes and elevation in AIDS dementia. Proc. Natl. Acad. Sci. U. S. A. 95, 3117–3121.

da Cunha, A., Rausch, D.M., Eiden, L.E., 1995. An early increase in somatostatin mRNA expression in the frontal cortex of rhesus monkeys infected with simian immunodeficiency virus. Proc. Natl. Acad. Sci. U. S. A. 92, 1371–1375.

Depboylu, C., Reinhart, T.A., Schwaeble, W.J., Mitsuya, H., Eiden, L.E., Weihe, E., 2001. Brain C1q is increased in SIV infection in the rhesus macaque, and is directly related to brain virus burden. Soc. Neurosci. Abstr. 27:1745, 657.16.

Depboylu, C., Reinhart, T.A., Takikawa, O., Imai, Y., Maeda, H., Mitsuya, H., Rausch, D., Eiden, L.E., Weihe, E., 2004. Brain virus burden and indoleamine-2,3-dioxygenase during lentiviral infection of rhesus monkey are concomitantly lowered by 6-chloro-2′,3′-dideoxyguanosine. Eur. J. Neurosci. 19, 2997–3005.

Dickson, D.W., 1986. Multinucleated giant cells in acquired immunodeficiency syndrome encephalopathy. Arch. Pathol. Lab. Med. 110, 967–968.

Dietzschold, B., Schwaeble, W., Schäfer, M.K.-H., Petry, F., Zheng, Y., Fink, T., Loos, M., Weihe, E., 1995. The expression of C1q, a subcomponent of the rat complement system is dramatically enhanced in brains of rats with either Borna disease or experimental allergic encephalomyelitis. J. Neurol. Sci. 130, 11–16.

Ebenbichler, C.F., Thielens, N.M., Vornhagen, R., Marschan, P., Arlaud, G.J., Dierich, M.P., 1991. Human immunodeficiency virus type 1 activates the classical pathway of complement by direct C1 binding through specific sites in the transmembrane glycoprotein gp 41. J. Exp. Med. 174, 1417–1424.

Eggleton, P., Tenner, A.J., Reid, K.B., 2000. C1q receptors. Clin. Exp. Immunol. 120, 406–412.

Farkas, I., Takahashi, M., Fukuda, A., Yamamoto, N., Akatsu, H., Baranyi, L., Tateyama, H., Yamamoto, T., Okada, N., Okada, H., 2003. Complement C5a receptor-mediated signaling may be involved in neurodegeneration in Alzheimer's disease. J. Immunol. 170, 5764–5771.

Fonseca, M.I., Kawas, C.H., Troncoso, J.C., Tenner, A.J., 2004. Neuronal localization of C1q in preclinical Alzheimer's disease. Neurobiol. Dis. 15, 40–46.

Fuchs, D., Moller, A.A., Reibnegger, G., Stockle, E., Werner, E.R., Wachter, H., 1990. Decreased serum tryptophan in patients with HIV-1 infection correlates with increased serum neopterin and with neurologic/psychiatric symptoms. Acquir. Immune Defic. Syndr. 3, 873–876.

Fujii, Y., Mukai, R., Mori, K., Akari, H., Otani, I., Ono, F., Kojima, E., Takasaka, M., Machida, M., Murakami, K., Yoshikawa, Y., 1997a. Efficacy of 6-chloro-2′,3′-dideoxyguanosine (6-Cl-ddG) on rhesus macaque monkeys chronically infected with simian immunodeficiency virus (SIVmac239). J. Acquir. Immune Defic. Syndr. Hum. Retrovirol. 16, 313–317.

Fujii, Y., Mukai, R., Murayama, Y., Akari, H., Machida, M., Mori, K., Takasaka, M., Murakami, K., Yoshikawa, Y., 1997b. Efficacy of 6-chloro-2′,3′-dideoxyguanosine (6-Cl-ddG) on an ARC/AIDS rhesus macaque (*Macaca mulatta*) infected with simian immunodeficiency virus. Exp. Anim. 46, 83–87.

Fujii, Y., Mukai, R., Akari, H., Machida, M., Mori, K., Takasaka, M., Kojima, E., Murakami, K., Yoshikawa, Y., 1998. Antiviral effects of 6-chloro-2′,3′-dideoxyguanosine in rhesus monkeys acutely infected with simian immunodeficiency virus. Antivir. Chem. Chemother. 9, 85–92.

Ghebrehiwet, B., Kew, R.R., Gruber, B.L., Marchese, M.J., Peerschke, E.I., Reid, K.B., 1995. Murine mast cells express two types of C1q receptors that are involved in the induction of chemotaxis and chemokinesis. J. Immunol. 155, 2614–2619.

Glass, J.D., Fedor, H., Wesselingh, S.L., McArthur, J.C., 1995. Immunocytochemical quantitation of human immunodeficiency virus in the brain: correlations with dementia. Ann. Neurol. 38, 755–762.

Gulevich, S.J., McCutchan, J.A., Thal, L.J., Kirson, D., Durand, D., Wallace, M., Mehta, P., Heyes, M.P., Grant, I., 1993. Effect of antiretroviral therapy on the cerebrospinal fluid of patients seropositive for the human immunodeficiency virus. J. Acquir. Immune Defic. Syndr. 6, 1002–1007.

Hawkins, M.E., Mitsuya, H., McCully, C.L., Godwin, K., Murakami, K., Poplack, D.G., Balis, F.M., 1995. Plasma and cerebrospinal fluid pharmacokinetics of dideoxypurine nucleoside analogs in rhesus monkeys. Antimicrob. Agents Chemother. 39, 1259–1264.

Head, E., Azizeh, B.Y., Lott, I.T., Tenner, A.J., Cotman, C.W., Cribbs, D.H., 2001. Complement association with neurons and beta-amyloid deposition in the brains of aged individuals with down syndrome. Neurobiol. Dis. 8, 252–265.

Heyes, M.P., Rubinow, D., Lane, C., Markey, S.P., 1989. Cerebrospinal fluid quinolinic acid concentrations are increased in acquired immune deficiency syndrome. Ann. Neurol. 26, 275–277.

Kato, T., Hirano, A., Llena, J.F., Dembitzer, H.M., 1987. Neuropathology of the acquired immune deficiency syndrome (AIDS) in 53 autopsy cases with particular emphasis on microglial nodules and multinucleated giant cells. Acta Neuropathol. 73, 287–294.

Kent, K.A., Rud, E., Cororan, T., Powell, C., Thiriart, C., Collignon, C., Stott, E.J., 1992. Identification of two neutralizing and eight non-neutralizing epitopes on simian immunodeficiency virus envelope using monoclonal antibodies. AIDS Res. Hum. Retroviruses 8, 1147–1151.

Kishore, U., Reid, K.B., 2000. C1q: structure, function and receptors. Immunopharmacology 49, 159–170.

Klein, M.A., Kaeser, P.S., Schwarz, P., Weyd, H., Xenarios, I., Zinkernagel, R.M., Carroll, M.C., Verbeek, J.S., Botto, M., Walport, M.J., Molina, H., Kalinke, U., Acha-Orbea, H., Aguzzi, A., 2001. Complement facilitates early prion pathogenesis. Nat. Med. 7, 488–492.

Kovacs, G.G., Gasque, P., Strobel, T., Lindeck-Pozza, E., Strohschneider, M., Ironside, J.W., Budka, H., Guentchev, M., 2004. Complement activation in human prion disease. Neurobiol. Dis. 15, 21–28.

Kuna, P., Iyer, M., Peerschke, E.I., Kaplan, A.P., Reid, K.B., Ghebrehiwet,

B., 1996. Human C1q induces eosinophil migration. Clin. Immunol. Immunopathol. 81, 48–54.
Lane, J.H., Sasseville, V.G., Smith, M.O., Vogel, P., Pauley, D.R., Heyes, M.P., Lackner, A.A., 1996. Neuroinvasion by simian immunodeficiency virus coincides with increased numbers of perivascular macrophages/microglia and intrathecal immune activation. J. Neurovirol. 2, 423–432.
Leigh, L.E., Ghebrehiwet, B., Perera, T.P., Bird, I.N., Strong, P., Kishore, U., Reid, K.B., Eggleton, P., 1998. C1q-mediated chemotaxis by human neutrophils: involvement of gClqR and G-protein signalling mechanisms. Biochem. J. 330, 247–254.
Li, Q., Eiden, L.E., Cavert, W., Reinhart, T.A., Rausch, D.M., Murray, E.A., Weihe, E., Haase, A.T., 1999. Increased expression of nitric oxide synthase and dendritic injury in simian immunodeficiency virus encephalitis. J. Hum. Virol. 2, 139–145.
Lifson, J.D., Reyes, G.R., McGrath, M.S., Stein, B.S., Engelmann, E.G., 1986. AIDS retrovirus induced cytopathology: giant cell formation and involvement of CD4 antigen. Science 232, 1123–1127.
Lipton, S.A., Sucher, N.J., Kaiser, P.K., Dreyer, E.B., 1991. Synergistic effects of HIV coat protein and NMDA receptor-mediated neurotoxicity. Neuron 7, 111–118.
Look, M.P., Altfeld, M., Kreuzer, K.A., Riezler, R., Stabler, S.P., Allen, R.H., Sauerbruch, T., Rockstroh, J.K., 2000. Parallel decrease in neurotoxin quinolinic acid and soluble tumor necrosis factor receptor p75 in serum during highly active antiretroviral therapy of HIV type 1 disease. AIDS Res. Hum. Retroviruses 16, 1215–1221.
Luabeya, M.-K., Dallasta, L.M., Achim, C.L., Pauza, C.D., Hamilton, R.L., 2000. Blood–brain barrier disruption in simian immunodeficiency virus encephalitis. Neuropathol. Appl. Neurobiol. 26, 454–462.
Luthert, P.J., Montgomery, M.M., Dean, A.F., Cook, R.W., Baskerville, A., Lantos, P.L., 1995. Hippocampal neuronal atrophy occurs in rhesus macaques following infection with simian immunodeficiency virus. Neuropathol. Appl. Neurobiol. 21, 529–534.
Lynch, N.J., Willis, C.L., Nolan, C.C., Roscher, S., Fowler, M.J., Weihe, E., Ray, D.E., Schwaeble, W.J., 2004. Microglial activation and increased synthesis of complement component C1q precedes blood–brain barrier dysfunction in rats. Mol. Immunol. 40, 709–716.
Montefiori, D.C., Robinson, W.E., Hirsch, V.M., Modliszewski, A., Mitchell, W.M., Johnson, P.R., 1990. Antibody-dependent enhancement of simian immnodeficiency virus (SIV) infection in vitro by plasma from SIV-infected rhesus macaques. J. Virol. 64, 113–119.
Mulligan, M.S., Schmid, E., Till, G.O., Hugli, T.E., Friedl, H.P., Roth, R.A., Ward, P.A., 1997. C5a-dependent up-regulation in vivo of lung vascular P-selectin. J. Immunol. 158, 1857–1861.
Murray, E.A., Rausch, D.M., Lendvay, J., Sharer, L.R., Eiden, L.E., 1992. Cognitive and motor impairments associated with SIV infection in rhesus monkeys. Science 255, 1246–1249.
Overholser, E.D., Coleman, G.D., Bennett, J.L., Casaday, R.J., Zink, M.C., Barber, S.A., Clements, J.E., 2003. Expression of simian immunodeficiency virus (SIV) nef in astrocytes during acute and terminal infection and requirement of nef for optimal replication of neurovirulent SIV in vitro. J. Virol. 77, 6855–6866.
Perricone, R., Fontana, L., De Carolis, C., Carini, C., Sirianni, M.C., Aiuti, F., 1987. Evidence for activation of complement in patients with AIDS-related complex (ARC) and/or lymphadenopathy syndrome (LAS). Clin. Exp. Immunol. 70, 500–507.
Power, C., Gill, M.J., Johnson, R.T., 2002. Progress in clinical neurosciences: the neuropathogenesis of HIV infection: host–virus interaction and the impact of therapy. Can. J. Neurol. Sci. 29, 19–32.
Reinhart, T.A., Rogan, M.J., Huddleston, D., Rausch, D.M., Eiden, L.E., Haase, A.T., 1997. Simian immunodeficiency virus burden in tissues and cellular compartments during clinical latency and AIDS. J. Infect. Dis. 176, 1198–1208.
Roberts, E.S., Zandonatti, M.A., Watry, D.D., Madden, L.J., Henriksen, S.J., Taffe, M.A., Fox, H.S., 2003. Induction of pathogenic sets of genes in macrophages and neurons in NeuroAIDS. Am. J. Pathol. 162, 2041–2057.
Robinson Jr., W.E., Montefiori, D.C., Mitchell, W.M., 1988. Antibody-dependent enhancement of human immunodeficiency virus type 1 infection. Lancet 1, 790–794.
Robinson Jr., W.E., Montefiori, D.C., Mitchell, W.M., Prince, A.M., Alter, H.J., Dreesmann, G.R., Eichberg, J.W., 1989. Antibody-dependent enhancement of human immunodeficiency virus type 1 (HIV-1) infection in vitro by serum from HIV-1-infected and passively immunized chimpanzees. Proc. Natl. Acad. Sci. U. S. A. 86, 4710–4714.
Robinson, W.E., Montefiori, D.C., Mitchell, W.M., 1990. Complement-mediated antibody-dependent enhancement of HIV-1 infection requires CD4 and complement receptors. Virology 175, 600–604.
Rohrenbeck, A.M., Bette, M., Hooper, D.C., Nyberg, F., Eiden, L.E., Dietzschold, B., Weihe, E., 1999. Upregulation of COX-2 and CGRP expression in resident cells of the Borna disease virus-infected brain is dependent upon inflammation. Neurobiol. Dis. 6, 15–34.
Rostagno, A., Revesz, T., Lashley, T., Tomidokoro, Y., Magnotti, L., Braendgaard, H., Plant, G., Bojsen-Moller, M., Holton, J., Frangione, B., Ghiso, J., 2002. Complement activation in chromosome 13 dementias. Similarities with Alzheimer's disease. J. Biol. Chem. 277, 49782–49790.
Saito, Y., Sharer, L.R., Epstein, L.G., Michaels, J., Mintz, M., Louder, M., Golding, K., Cvetkovich, T.A., Blumberg, B.M., 1994. Overexpression of nef as a marker for restricted HIV-1 infection of astrocytes in postmortem pediatric central nervous tissues. Neurology 44, 474–481.
Schäfer, M.K.-H., Day, R., 1994. In situ hybridization techniques to study processing enzyme expression at the cellular level. Methods Neurosci. 23, 16–44.
Schäfer, M.K.-H., Herman, J.P., Watson, S.J., 1992. In situ hybridization immunohistochemistry. In: London, D. (Ed.), Imaging Drug Action in the Brain. CRC Press, Boca Raton, p. 337.
Schäfer, M.K.-H., Schwaeble, W., Post, C., Salvati, P., Calabresi, M., Sim, R.B., Petry, F., Loos, M., Weihe, E., 2000. Complement C1q is dramatically up-regulated in brain microglia in response to transient global cerebral ischemia. J. Immunol. 164, 5446–5452.
Sellar, G.C., Blake, D.J., Reid, K.B., 1991. Characterization and organization of the genes encoding the A-, B- and C-chains of human complement subcomponent C1q. The complete derived amino acid sequence of human C1q. Biochem. J. 274, 481–490.
Senaldi, G., Peakman, M., McManus, T., Davies, E.T., Tee, D.E., Vergani, D., 1990. Activation of the complement system in human immundeficiency virus infection: relevance of the classical pathway to pathogenesis and disease severity. J. Infect. Dis. 162, 1227–1232.
Shirasaka, T., Murakami, K., Ford, H., Kelley, J., Yoshioka, H., Kojima, E., Aoki, S., Driscoll, J.S., Broder, S., Mitsuya, H., 1990. Halogeneted congeners of 2′,3′-dideoxypurine nucleosides active against HIV in vitro: a new class of lipophilic prodrugs. Proc. Natl. Acad. Sci. U. S. A. 87, 9426–9430.
Singhrao, S., Neal, J., Gasque, P., Morgan, B., Newman, G., 1996. Role of complement in the aetiology of Pick's disease? J. Neuropathol. Exp. Neurol. 55, 578–593.
Smyth, M.D., Cribbs, D.H., Tenner, A.J., Shankle, W.R., Dick, M., Kesslak, J.P., Cotman, C.W., 1994. Decreased levels of C1q in cerebrospinal fluid of living Alzheimer patients correlate with disease state. Neurobiol. Aging 15, 609–614.
Sölder, B.M., Schulz, T.F., Hengster, P., Löwer, J., Larcher, C., Bitterlich, G., Kurth, R., Wachter, H., Dierich, M.P., 1989. HIV and HIV-infected cells differentially activate the human complement system independent of antibody. Immunol. Lett. 22, 135–145.
Speth, C., Kacani, L., Dierich, M.P., 1997. Complement receptors in HIV infection. Immunol. Rev. 159, 49–67.
Speth, C., Dierich, M.P., Gasque, P., 2002. Neuroinvasion by pathogens: a key role of the complement system. Mol. Immunol. 38, 669–679.
Speth, C., Williams, K., Hagleitner, M., Westmoreland, S., Rambach, G., Mohsenipour, I., Schmitz, J., Würzner, R., Lass-Flörl, C., Stoiber, H., Dierich, M.P., Maier, H., 2004. Complement synthesis and activation in the brain of SIV-infected monkeys. J. Neuroimmunol. 151, 45–54.
Tornatore, C., Chandra, R., Berger, J.R., Major, E.O., 1994. HIV-1 infection

of subcortical astrocytes in the pediatric central nervous system. Neurology 44, 481–487.

Tremblay, M., Meloche, S., Sekaly, R.P., Wainberg, M.A., 1990. Complement receptor 2 mediated enhancement of human immunodeficiency virus type 1 infection in Epstein–Barr virus carrying B cells. J. Exp. Med. 171, 1791–1796.

van den Berg, R.H., Faber-Krol, M.C., Sim, R.B., Daha, M.R., 1998. The first subcomponent of complement, C1q, triggers the production of IL-8, IL-6, and monocyte chemoattractant peptide-1 by human umbilical vein endothelial cells. J. Immunol. 161, 6924–6930.

Velazquez, P., Cribbs, D., Poulos, T., Tenner, A., 1997. Aspartate residue 7 in amyloid β-protein is critical for classical complement pathway activation: implications for Alzheimer's disease pathogenesis. Nat. Med. 3, 77–91.

Wajgt, A., Gorny, M., Szczechowski, L., Grzybowski, G., Ochudlo, S., 1989. Effect of immunosuppressive therapy on humoral immune response in multiple sclerosis. Acta Med. Pol. 30, 121–128.

Walsh, M.J., Murray, J.M., 1998. Dual implication of 2′,3′-cyclic nucleotide 3′-posphodiesterase as major autoantigen and C3-complement-binding protein in the pathogenesis of multiple sclerosis. J. Clin. Invest. 101, 1923–1931.

Weihe, E., Nohr, D., Sharer, L., Murray, E., Rausch, D.M., Eiden, L.E., 1993. Cortical astrocytosis in juvenile rhesus monkeys infected with simian immunodeficiency virus. NeuroReport 4, 263–266.

Whaley, K., Schwaeble, W., 1997. Complement and complement deficiencies. Semin. Liver Dis. 17, 297–310.

Williams, K.C., Hickey, W.F., 1995. Traffic of hematogenous cells through the central nervous system. Curr. Top. Microbiol. Immunol. 202, 221–245.

Williams, A.E., Lawson, L.J., Perry, V.H., Fraser, H., 1994. Characterization of the microglial response in murine scrapie. Neuropathol. Appl. Neurobiol. 20, 47–55.

Williams, K.C., Corey, S., Westmoreland, S.V., Pauley, D., Knight, H., deBakker, C., Alvarez, X., Lackner, A.A., 2001. Perivascular macrophages are the primary cell type productively infected by simian immunodeficiency virus in the brains of macaques: implications for the neuropathogenesis of AIDS. J. Exp. Med. 193, 905–915.

Wyss-Coray, T., Yan, F., Lin, A.H., Lambris, J.D., Alexander, J.J., Quigg, R.J., Masliah, E., 2002. Prominent neurodegeneration and increased plaque formation in complement-inhibited Alzheimer's mice. Proc. Natl. Acad. Sci. U. S. A. 99, 10837–10842.

Yamada, T., Moroo, I., Koguchi, Y., Asahina, M., Hirayama, K., 1994. Increased concentration of C4d complement protein in cerebrospinal fluids in progressive nuclear palsy. Acta Neurol. Scand. 89, 42–46.

THE JOURNAL OF BIOLOGICAL CHEMISTRY VOL. 281, NO. 2, pp. 1241–1250, January 13, 2006
Printed in the U.S.A.

Altered HIV-1 Gag Protein Interactions with Cyclophilin A (CypA) on the Acquisition of H219Q and H219P Substitutions in the CypA Binding Loop*

Received for publication, May 31, 2005, and in revised form, November 7, 2005 Published, JBC Papers in Press, November 7, 2005, DOI 10.1074/jbc.M505920200

Hiroyuki Gatanaga[‡1], Debananda Das[‡], Yasuhiro Suzuki[‡§], Damaris D. Yeh[‡], Khaja A. Hussain[¶], Arun K. Ghosh[¶], and Hiroaki Mitsuya[‡§2]

From the [‡]Experimental Retrovirology Section, HIV and AIDS Malignancy Branch, NCI, National Institutes of Health, Bethesda, Maryland 20892, the [§]Departments of Hematology and Infectious Diseases, Kumamoto University School of Medicine, Kumamoto 860, Japan, and the [¶]Department of Chemistry, University of Illinois, Chicago, Illinois 60607

HIV-1 Gag protein interaction with cyclophilin A (CypA) is critical for viral fitness. Among the amino acid substitutions identified in Gag noncleavage sites in HIV-1 variants resistant to protease inhibitors, H219Q (Gatanaga, H., Suzuki, Y., Tsang, H., Yoshimura, K., Kavlick, M. F., Nagashima, K., Gorelick, R. J., Mardy, S., Tang, C., Summers, M. F., and Mitsuya, H. (2002) *J. Biol. Chem.* 277, 5952–5961) and H219P substitutions in the viral CypA binding loop confer the greatest replication advantage to HIV-1. These substitutions represent polymorphic amino acid residues. We found that the replication advantage conferred by these substitutions was far greater in CypA-rich MT-2 and H9 cells than in Jurkat cells and peripheral blood mononuclear cells (PBM), both of which contained less CypA. High intracellular CypA content in H9 and MT-2 cells, resulting in excessive CypA levels in virions, limited wild-type HIV-1 (HIV-1_{WT}) replication and H219Q introduction into HIV-1 (HIV-1_{H219Q}), reduced CypA incorporation of HIV-1, and potentiated viral replication. H219Q introduction also restored the otherwise compromised replication of HIV-1_{P222A} in PBM, although the CypA content in HIV-$1_{H219Q/P222A}$ was comparable with that in HIV-1_{P222A}, suggesting that H219Q affected the conformation of the CypA-binding motif, rendering HIV-1 replicative in a low CypA environment. Structural modeling analyses revealed that although hydrogen bonds are lost with H219Q and H219P substitutions, no significant distortion of the CypA binding loop of Gag occurred. The loop conformation of HIV-1_{P222A} was found highly distorted, although H219Q introduction to HIV-1_{P222A} restored the conformation of the loop close to that of HIV-1_{WT}. The present data suggested that the effect of CypA on HIV-1 replicative ability is bimodal (both high and low CypA content limits HIV-1 replication), that the conformation of the CypA binding region of Gag is important for viral fitness, and that the function of CypA is to maintain the conformation.

Combination antiretroviral therapy has brought about improved quality of life and extended survival in patients with HIV-1[3] infection. However, the emergence of HIV-1 variants resistant to anti-HIV-1 therapeutic agents, including reverse transcriptase inhibitors and protease inhibitors (PIs), has limited the efficacy of chemotherapy (1). HIV-1 develops resistance mainly by substituting amino acids in the target viral enzyme or component; however, recent studies have revealed that certain polymorphic amino acid residues also contribute to the viral resistance (2, 3). We recently found that multiple amino acid substitutions emerged in noncleavage sites of the Gag protein, which were associated with the development of HIV-1 resistance against PIs (4). Among such amino acid substitutions, H219Q, occurring in the cyclophilin A (CypA) binding loop in the p24 Gag protein, conferred the greatest replication advantage on HIV-1 (4). CypA binds to p24 Gag protein, resulting in the packaging of ~200 copies of CypA into each HIV-1 virion (5, 6), and is thought to perform an essential role early in the HIV-1 replication cycle (7, 8), perhaps by destabilizing the capsid (p24 Gag protein) shell during viral entry and uncoating (9) and/or by performing an additional chaperon function, facilitating correct capsid condensation during viral maturation (10, 11).

In the present study, we asked how H219Q and H219P substitutions occurring within the viral CypA binding loop conferred replication advantage to HIV-1, and we examined whether these substitutions affected the conformation and interaction of p24 Gag protein and CypA during HIV-1 propagation in various host cells. We also attempted to better understand the functional role of CypA in HIV-1 replication. To that end, we determined the virological and biochemical properties of a variety of recombinant infectious clones and their CypA contents. We also carried out molecular modeling analyses of the wild-type and mutated p24 Gag complex with CypA. The data demonstrate that both H219Q and H219P enhance HIV-1 replication by reducing viral CypA contents in daughter virions as produced in CypA-rich cells, but not in cells that has a low CypA content. We suggest that the effect of CypA on HIV-1 replicative ability is bimodal, both high and low contents of CypA limit HIV-1 replication. The data also suggest that the conformation of p24 Gag is strongly correlated with viral fitness.

EXPERIMENTAL PROCEDURES

Antiviral Agents—Three PIs, KNI-272, JE-2147, and UIC-94003, were synthesized as described previously (12–16). Three newly synthesized PIs, UIC-00041, UIC-00142, and UIC-00145 (Fig. 1), were also

* This work was supported in part by the Intramural Research Program of the NCI, Center for Cancer Research, National Institutes of Health, in part by National Institutes of Health Grant GM 53386 (to A. K. G.), in part by Research for the Future Program Grant JSPS-RFTF 97L00705 from the Japan Society for the Promotion of Science (to H. M.), a grant-in-aid for scientific research (priority areas) from the Ministry of Education (to H. M.), a grant from the Culture, Sports, Sciences, and Technology of Japan (Monbu-Kagakusho) (to H. M.), and a grant for the promotion of AIDS research from the Ministry of Health Welfare and Labor of Japan (Kosei-Rohdosho) (to H. M.). The costs of publication of this article were defrayed in part by the payment of page charges. This article must therefore be hereby marked "*advertisement*" in accordance with 18 U.S.C. Section 1734 solely to indicate this fact.

[1] Present address: AIDS Clinical Center, International Medical Center of Japan, Tokyo 162-8655, Japan.

[2] To whom correspondence should be addressed: Experimental Retrovirology Section, HIV and AIDS Malignancy Branch, NCI, National Institutes of Health, Bldg. 10, Rm. 5A11, 9000 Rockville Pike, Bethesda, MD 20892. Tel.: 301-496-9238; Fax: 301-402-0709; E-mail: hmitsuya@helix.nih.gov.

[3] The abbreviations used are: HIV-1, human immunodeficiency virus, type 1; PBM, peripheral blood mononuclear cell; CHRA, competitive HIV-1 replication assay; CypA, cyclophilin A; PI, protease inhibitor; PHA, phytohemagglutinin; CsA, cyclosporin A; CA, capsid; WT, wild type.

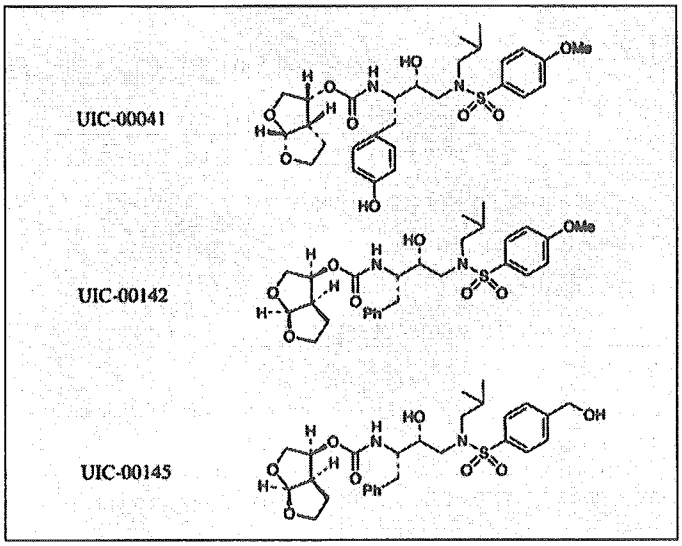

FIGURE 1. **Structures of UIC-00041, UIC-00142, and UIC-00145.**

synthesized by Ghosh and Hussain,[4] and the procedures for the synthesis will be published elsewhere.

Generation of HIV-1 Variants Resistant to PIs—The wild-type infectious clone, HIV-1_{WT}, produced by COS-7 cells transfected with pHIV-1_{NL4-3} was propagated in human $CD4^+$ MT-2 or H9 cells in the presence of increasing concentrations of an antiretroviral agent as described previously (4, 14, 16). Briefly, MT-2 or H9 cells (5×10^5) were exposed to wild-type HIV-1_{NL4-3} and cultured in the presence of each PI at initial concentrations of 0.0005–0.03 μM. When the virus began to propagate in the presence of the drug, the drug concentration was increased. This selection was carried out for a total of 27–80 passages. For the generation of JE-2147-resistant virus, an infectious clone carrying I84V substitution in the protease (HIV-1_{I84V}) was employed instead of HIV-1_{WT} (14). Proviral DNA in the lysates of HIV-1-infected cells of the last passage was sequenced as indicated (4).

Generation of Recombinant HIV-1 Clones—To generate HIV-1 clones carrying the desired mutations, the site-directed mutagenesis was performed, and the mutation-containing genomic fragments thus obtained were introduced to pHIV-1_{NLSma} as described previously (4). An infectious clone containing P222A mutation in Gag was generated using a plasmid kindly provided by Drs. D. Braaten and J. Luban (5). Each recombinant plasmid was transfected into COS-7 cells, and the obtained infectious virions were harvested 48 h after transfection and stored at −80 °C until use (4).

Replication Kinetic Assay—MT-2, H9, Jurkat cells (10^5), or phytohemagglutinin-stimulated peripheral blood mononuclear cells (PHA-PBM: 5×10^6) were exposed to each infectious virus preparation (500 blue-cell-forming units defined in the MAGI assay) (17) for 12 h, washed twice with phosphate-buffered saline, and cultured in 5 ml of complete medium in the presence or absence of cyclosporin A (CsA). Culture supernatants (200 μl) were harvested every other day or every 4 days, and p24 Gag amounts were determined using a commercially available radioimmunoassay kit (PerkinElmer Life Sciences). An enzyme-linked immunosorbent assay kit (Beckman Instruments, Fullerton, CA) was also used for the determination of p24 Gag amounts as needed.

Competitive HIV-1 Replication Assay Using PHA-PBM—In order to compare the replication rates of infectious HIV-1 clones, the competitive HIV-1 replication assay (CHRA) was performed as described previously (18) with some modifications. In brief, PHA-PBMs (5×10^6) were exposed to various mixtures of the paired infectious clones to be examined for their replicative ability and were cultured for the indicated times. Every 7 days, the supernatants of the virus co-culture were transferred to freshly prepared uninfected PHA-PBM cultures. DNA purified from the cells harvested at each passage was subjected to direct DNA sequencing of the HIV-1 genome, and viral population changes were evaluated based on relative peak heights in the electropherogram (18).

Western Blot Analysis—For the analysis of cellular CypA contents, MT-2 cells, H9 cells, Jurkat cells, or PHA-PBMs were lysed with lysis buffer (4), and the amounts of lysates were normalized with cell numbers or total protein contents using a bicinchoninic acid protein assay kit (Pierce). For the analysis of virion-associated CypA, the culture supernatants of chronically HIV-1-infected H9 or Jurkat cells were centrifuged and passed through a 0.22-μm pore-size filter to remove cellular debris; the filtrates were normalized with p24 contents measured with radioimmunoassay and were ultracentrifuged to pellet virions (4). The pelleted virions were lysed in lysis buffer. The resultant samples were processed with SDS-polyacrylamide gradient gels, and CypA was visualized by SuperSignalWestPico (Pierce) using anti-CypA antiserum (Biomol, Plymouth Meeting, PA). An anti-p24 Gag antiserum (Advanced Biotechnologies, Inc., Columbia, MD) served as a control to ensure that appropriate amounts of the samples were loaded. The signal density of CypA and p24 Gag was analyzed on a Windows computer by using the ImageJ Program (developed at National Institutes of Health, rsb.info.nih.gov/ij/) as published previously (19).

Molecular Modeling of the $p24_{CA151}$-CypA Complex with p24 Amino Acid Substitutions—The crystal structure of human CypA that was bound to the amino-terminal domain of p24 Gag (capsid residues 1–151 (CA_{151}), Protein Data Bank code 1AK4) (9) was analyzed to determine the changes with H219Q or H219P substitution. There were two CA-CypA complexes in the structure. Chain A of CypA and chain D of CA form one complex and were retained for the calculation. Identical results should be obtained with the other complex (chain B of CypA and chain C of CA) because the conformations of both CypA and CA in these complexes are quite similar. Structural modifications, visualization, and analysis were performed utilizing the Maestro interface from Schrödinger (Maestro 7.0, Schrödinger, LLC, New York). OPLS2003 force field (20) as implemented in MacroModel 9.0 (MacroModel, version 9.0, Schrödinger, LLC, New York) was used for minimizing mutated structures and for carrying out molecular dynamics calculations. OPLS2003 uses an enhanced version of the widely used OPLS-AA force field and has improved parameters for peptides. It was verified that the force field had high quality bond stretching, bending, and torsional parameters. Charges were taken from the force field. Molecular dynamics calculations were carried out on the wild-type complex and on the mutated structures. The structures were initially minimized for 2500 iterations. A constant temperature of 300 K and SHAKE constraints for bonds to hydrogens were used. The GB/SA continuum solvation model, with water as the solvent, was used (21). While calculating nonbonded interactions, cut-off distances of 8 and 20 Å were used for van der Waals and electrostatic interactions, respectively. Using a time step of 2 fs, the structures were equilibrated for 20 ps, and the simulation was carried out for 1 ns. Structures were monitored at intervals of every 50 ps. Calculations were carried out on an SGI Origin 3400 computer platform. For the wild type and for each mutant structure, 1-ns molecular dynamics calculation takes about 11 days under the stated conditions on this high performance computational platform.

[4] A. K. Ghosh and K. A. Hussain, personal communication.

TABLE 1

Amino acid substitutions identified in the protease and p24 Gag protein of HIV-1 variants selected against PI

Amino acid substitutions listed are based on the amino acid sequences deduced from the nucleotide sequence of the protease-encoding and the entire Gag-encoding genes of each HIV-1 selected against an indicated PI.

PI	Strain	Cell	Passage	Amino acid substitutions identified in	
				Protease	p24
KNI-272	HIV-1_{NL4-3}[a]	MT-2	27	V32I/M46I/V82I/I84V	H219Q
KNI-272	HIV-1_{LAI}	H9	55	V32I/L33F/K45I/F53L/A71V/I84V	H219Q
APV	HIV-1_{NL4-3}[a]	MT-2	31	L10F/V32I/M46I/I54M/A71V/I84V	H219Q
JE-2147	HIV-$1_{NL4-3/I84V}$[a]	MT-2	33	M46I/I47V/V82I/I84V	H219Q
UIC-94003	HIV-1_{NL4-3}[a]	MT-2	62	L10F/A28S/M46I/I50V/A71V	Q199H/H219Q
UIC-00041	HIV-1_{NL4-3}	MT-2	73	K43I/L63P/V82I	M200I/H219P
UIC-00142	HIV-1_{NL4-3}	MT-2	84	L10F/V32I/M46I/I84V	H219Q
UIC-00145	HIV-1_{NL4-3}	MT-2	80	L10F/V32I/M46I/I47A/K55N	H219Q

[a] PI-resistant HIV-1 variants described previously (4) are shown.

RESULTS

Amino Acid Substitutions Identified in p24 Gag Protein in HIV-1 Variants Resistant to PI—We have reported previously that several amino acid substitutions were seen in common in the Gag protein at noncleavage sites among HIV-1 variants that acquired *in vitro* a high multitude of resistance to PIs such as APV, JE-2147, KNI-272, and UIC-94003 (4). In an attempt to corroborate and extend our previous observations and to determine how often such amino acid substitutions develop in the Gag protein, we examined four more HIV-1 variants that were selected *in vitro* against various PIs, including three novel PIs, UIC-00041, UIC-00142, and UIC-00145. Table 1 depicts the properties of eight PI-resistant HIV-1 variants (including four HIV-1 variants reported previously). Seven of the eight variants were selected against PIs in MT-2 cells, although one variant was selected in H9 cells. The strains used were HIV-1_{NL4-3} and HIV-1_{LAI}, and 3–6-amino acid substitutions were identified in the protease. It was noted that all eight variants had in common an amino acid substitution at position 219 in p24 Gag protein, seven variants had H219Q substitution and one had H219P substitution. The His^{219} residue is located within the CypA binding loop and is thought to play a role in the p24 Gag interactions with CypA through a hydrogen bond and hydrophobic contact(s) (9). It is worth noting that when HIV-1_{NL4-3} was propagated in the absence of PI in MT-2 cells, the virus also acquired H219Q, V218M, or A224V mutation by passage 10 (4). It should be noted that two amino acids, Val^{218} and Ala^{224}, are also located within the CypA binding loop of the p24 Gag protein and are also known to interact with CypA through hydrophobic contacts (9). These data, taken together, strongly suggest that the amino acids interacting with CypA, in particular His^{219}, are prone to undergo substitutions under certain circumstances and are associated with viral replication fitness. Indeed, in the HIV Sequence Compendium 2000 (22), of 88 different HIV-1 strains, 65 had histidine at the position 219, whereas 13 had glutamine, and 4 had proline at the position 219, indicating that both Gln^{219} and Pro^{219} represent polymorphic amino acid residues. Hence, the present data suggest that these two polymorphic amino acids are associated with viral fitness and possibly to the acquisition of resistance to certain PIs.

Effects of Gag Mutations at Position 219 on HIV-1 Replication—In order to examine the effects of the Gag mutation at position 219 on HIV-1 replication, we generated two infectious HIV-1 clones, HIV-1_{H219Q} and HIV-1_{H219P}, and we assessed their virologic properties. In MT-2 cells, HIV-1_{H219Q} rapidly replicated compared with the wild-type HIV-$1_{WT(His-219)}$ (Fig. 2*A*), in agreement with our previous observation (4). HIV-1_{H219Q} also replicated more rapidly than HIV-1_{WT} in H9 cells (Fig. 2*B*). HIV-1_{H219P} replicated as rapidly as HIV-1_{H219Q}, suggesting that the amino acid at position 219 is critical for the replication fitness of HIV-1. When we examined the fitness of the three infectious clones (HIV-1_{WT}, HIV-1_{H219Q}, and HIV-1_{H219P}) in $CD4^+$ Jurkat cells and PHA-PBM, there was no significant difference seen in their replication fitness (Fig. 2, *C* and *D*).

Competitive HIV-1 Replication Assays for H219Q Mutation in PHA-PBM—As shown above, although HIV-1_{H219Q} exhibited a greater replication capability when propagated in MT-2 and H9 cells compared with HIV-1_{WT}, there was no apparent difference in the replication profiles of HIV-1_{H219Q} and HIV-1_{WT} as propagated in PHA-PBM (Fig. 2, *A*, *B* and *D*). In order to evaluate the possible biological relevance of the replication kinetic data generated by using immortalized and long term cultured MT-2 and H9 cells, we conducted a modified competitive HIV-1 replication assay (CHRA) (18), in which freshly prepared PHA-PBM served as host cells. HIV-1_{H219Q} readily and uniformly overgrew HIV-1_{WT} in CHRA regardless of three different ratios of paired clones used in the assay (Fig. 2, *E–G*). These data indicated that the H219Q substitution conferred replication advantages on HIV-1 when propagated in immortalized $CD4^+$ T cells as well as PHA-PBM. It should be noted, however, that the replication advantage of HIV-1 acquired with the H219Q substitution was limited in PHA-PBM and was detected only when assessed with CHRA.

MT-2 and H9 Cells Contain Greater Amounts of CypA—The Gag mutations H219Q and H219P conferred significant replication advantage on HIV-1 as propagated in MT-2 cells and H9 cells, but such advantage was limited in PHA-PBM. Considering that His^{219} is located within the CypA binding loop and that HIV-1 replication is known to be affected by intracellular CypA contents (6, 7), we examined intracellular CypA content in each cell preparation by using Western blot analysis. As shown in Fig. 3, *A* and *B*, the CypA contents in 10^4 MT-2 (relative density, 100%) and 10^4 H9 cells (79.6%) appeared to be greater than those in 5×10^4 Jurkat cells (55.4%) and 5×10^4 PHA-PBM (42.9%), suggesting that MT-2 and H9 cells contained 6–12 times as much CypA per cell as Jurkat cells and PHA-PBM. As normalized with total cellular protein amounts, the CypA content in 1 μg of MT-2 and H9 cellular protein preparations was comparable with that in 2–4 μg of Jurkat protein preparations and that in 4 μg of PHA-PBM protein, suggesting that the former two cell preparations contained 2–4-fold greater amounts of CypA per cellular protein than the latter two cell preparations. These data showed that MT-2 and H9 cells have greater CypA amounts than Jurkat T cells and PHA-PBM.

Decreased CypA Incorporation into HIV-1_{H219Q} Virions—Considering that the data from crystal structure analyses by Gamble *et al.* (9) of p24 Gag protein complexed with CypA showing that His^{219} binds to Asn^{71} and Gln^{111} of CypA through a hydrogen bond and hydrophobic contact(s), respectively, we postulated that H219Q and H219P substitutions cancel or weaken such hydrogen bonds, resulting in the reduction of p24 binding to CypA and of CypA incorporation into daughter virions, leading to increased HIV-1 replication in CypA-rich MT-2 and H9 cells. We then examined the virion-associated CypA amounts in

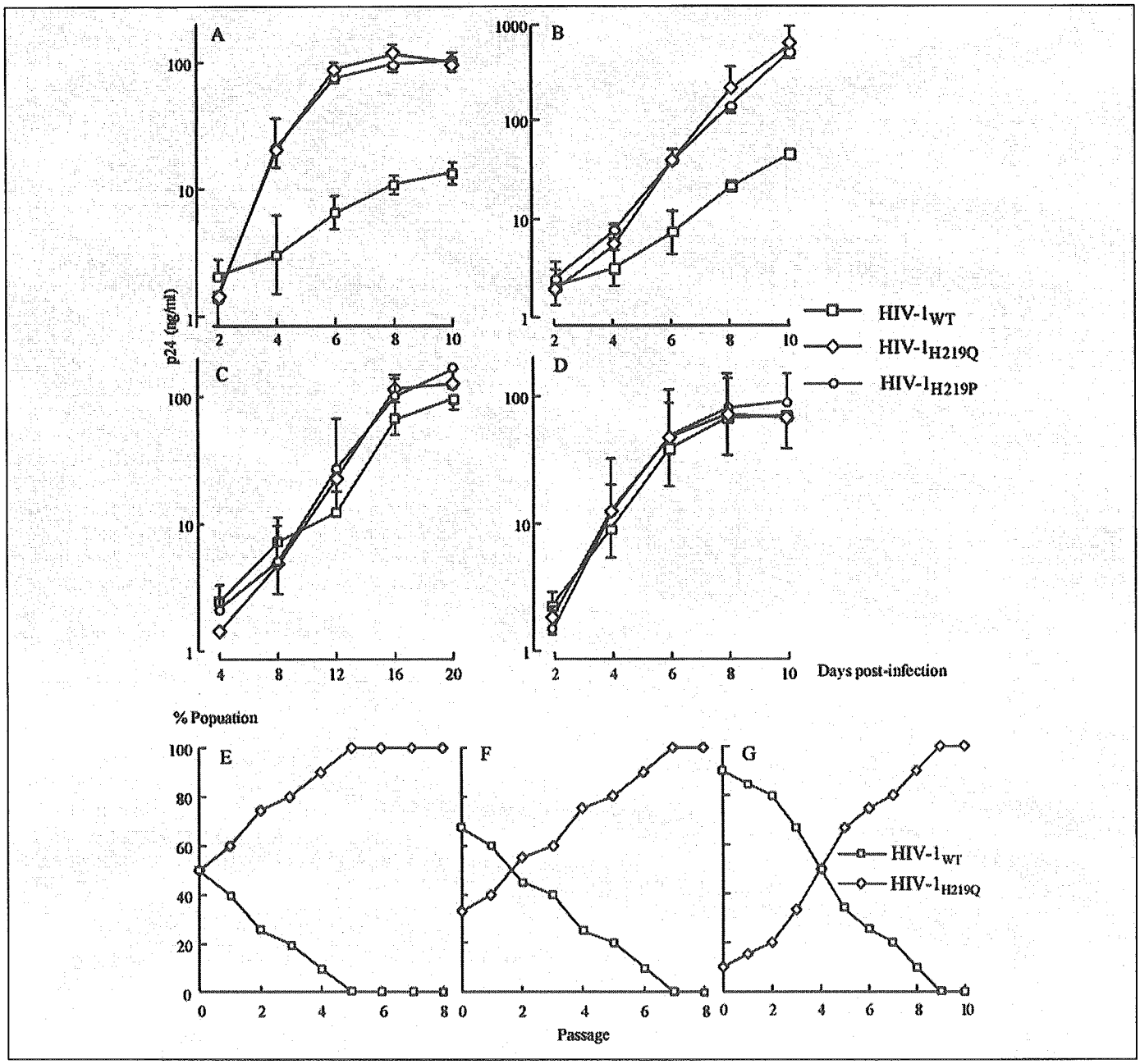

FIGURE 2. **Replication kinetics of HIV-1_{WT}, HIV-1_{H219Q}, and HIV-1_{H219P}.** MT-2 cells, H9 cells, Jurkat cells, and PHA-PBM (*A–D*, respectively) were exposed to each HIV-1 clone and cultured for the indicated numbers of passage. Virus replication was monitored by measuring the amounts of p24 Gag protein produced in the culture supernatants. The data shown represent geometric means (± 1 S.D.) of three independent experiments. Replication profiles of HIV-1_{WT} and HIV-1_{H219Q} in PHA-PBM were examined using CHRA (*E–G*). Two infectious HIV-1 clones to be compared for their fitness were mixed and propagated in PHA-PBM. The cell-free supernatant was transferred to fresh PHA-PBM every 7 days. The ratios of HIV-1_{WT} and HIV-1_{H219Q} at the initiation of the assay were 50:50, 67:33, and 90:10 (*E–G*, respectively). High molecular weight DNA extracted from infected cells at the end of each passage was subjected to nucleotide sequencing, and the proportions of His and Gln at position 219 in Gag protein were determined.

three infectious HIV-1 clones containing HIV-1_{WT}, HIV-1_{H219Q}, and HIV-1_{H219P}, employing Western blotting analysis using anti-p24 Gag and anti-CypA antisera. The culture supernatants of chronically HIV-1-infected H9 cells were prepared to contain the same amount of p24. The virions in each supernatant thus prepared were pelleted by ultracentrifugation and subsequently subjected to SDS-PAGE. Direct sequencing of cellular DNA confirmed that no unintended mutations developed during the culture. As shown in Fig. 3*C-1–3*, the experiment was performed three times. Percent densities of the CypA signal relative to each p24 Gag signal (making each signal 100%) were 11.1, 7.38, and 6.01% (Fig. 3*C-1*); 6.99, 4.99, and 4.71% (Fig. 3*C-2*), and 18.1, 12.0, and 11.2% (Fig. 3*C-3*) for HIV-1_{WT}/H9, HIV-1_{H219Q}/H9, and HIV-1_{H219P}/H9, respectively. These data demonstrated that H219Q and H219P substitutions increased HIV-1 replication in CypA-rich cells, which was associated with the substantial reduction of CypA incorporation into daughter virions.

p24 Gag Binding to CypA Affects HIV-1 Replication Kinetics—Yin *et al.* (23) have reported that the addition of CsA (0.5 μM) reduces CypA incorporation into daughter virions and increases replication rates of HIV-1_{1NL4-3} in H9 cells, suggesting that excessively high intracellular CypA contents may reduce HIV-1 replication rates. We then examined the effects of CsA on the replication rates of HIV-1_{WT} (Fig. 4, *A–D*) and HIV-1_{H219Q} (Fig. 4, *E–H*) in four different cell preparations.

In MT-2 and H9 cells, 0.5 μM CsA increased the replication rate of HIV-1_{WT}, whereas at a higher concentration (2.5 μM) its replication rate

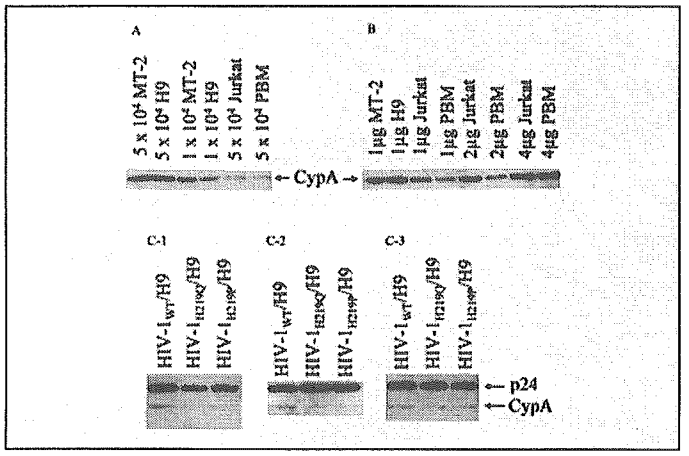

FIGURE 3. **MT-2 and H9 cells contain greater amounts of CypA than Jurkat cells and PHA-PBM, and HIV-1_{H219Q} and HIV-1_{H219P} virions contain reduced amounts of CypA than HIV-1_{WT} virions.** MT-2 cells, H9 cells, Jurkat cells, and PHA-PBM were lysed with lysis buffer, and the samples loaded were normalized by cell numbers or total protein contents. CypA was visualized with Western blotting analysis using anti-CypA antiserum (*A* and *B*). Percent CypA signal densities in 5×10^4 MT-2 cells, 5×10^4 H9 cells, 1×10^4 H9 cells, 5×10^4 Jurkat cells, and 5×10^4 PHA-PBM were 340.1, 387.4, 79.6, 55.4, and 42.9%, respectively, as compared with that in 1×10^4 MT-2 cells (serving as a standard to be 100%) (*A*). Percent CypA signal densities in 1 μg of H9 cells, 1 μg of Jurkat cells, 1 μg of PBM, 2 μg of Jurkat cells, 2 μg of PBMs, 4 μg of Jurkat cells, and 4 μg of PBMs were 155.2, 70.6, 35.0, 131.1, 59.5, 258.3, and 126.0%, respectively, as compared with that in 1 μg of MT-2 cells (serving as a standard to be 100%) (*B*). HIV-1 virions in the culture supernatants of chronically HIV-1-infected H9 cells were pelleted and subjected to Western blotting analysis for the determination of virion-associated CypA amounts using anti-p24 Gag and anti-CypA antisera. This experiment was performed three times (*C-1–3*). Percent densities of the CypA signal relative to each p24 Gag signal (making each p24 signal 100%) were 11.1, 7.38, and 6.01% in *C-1*; 6.99, 4.99, and 4.71% in *C-2*; and 18.1, 12.0, and 11.2% in *C-3* for HIV-1_{WT}/H9, HIV-1_{H219Q}/H9, and HIV-1_{H219P}/H9, respectively.

was reduced (Fig. 4, *A* and *B*), in agreement with the data by Yin *et al.* (23). In contrast, in Jurkat cells no increase in replication rate was seen, but rather CsA decreased HIV-1_{WT} replication in a dose-dependent manner (Fig. 4*C*). In PHA-PBM, CsA significantly decreased the replication rate of HIV-1_{WT}, and with 2.5 and 10 μM CsA, HIV-1_{WT} only poorly replicated (Fig. 4*D*). These data suggest that CsA (0.5 μM) can potentiate HIV-1_{WT} replication only in CypA-rich host cells. We further examined the effects of CsA on the replication of HIV-1_{H219Q} under the same conditions. In MT-2 and H9 cells (Fig. 4, *E* and *F*), no replication enhancement was seen with CsA added, but rather a reduced replication rate was observed in the presence of 0.5, 2.5, and 10 μM CsA. In Jurkat cells and PHA-PBM, the addition of CsA reduced the replication rate of HIV-1_{H219Q} as seen with HIV-1_{WT} (Fig. 4, *G* and *H*).

Taken together, the data suggest that the high intracellular CypA content in MT-2 and H9 cells was prohibitive to the replication of HIV-1_{WT} and that an appropriate concentration of CsA enhanced HIV-1_{WT} replication in CypA-rich cells by reduction of CypA incorporation into virions. In case of HIV-1_{H219Q}, however, H219Q already had reduced CypA incorporation into virions, and no enhanced replication was seen even in CypA-rich cells.

Effects of H219Q and P222A Substitutions on HIV-1 Replication—An amino acid substitution at position 222 from Pro to Ala (P222A) has been shown to substantially decrease the binding of p24 Gag protein to CypA and the CypA incorporation into daughter virions, causing reduced HIV-1 replication in Jurkat cells (6). As shown in Fig. 5, *A* and *B*, as examined in MT-2 and H9 cells, HIV-1_{1NL4-3} carrying P222A (HIV-1_{P222A}) had a relatively low replication rate compared with HIV-1_{WT} in both host cells. However, with the introduction of both H219Q and P222A substitutions, HIV-$1_{H219Q/P222A}$ acquired faster replication rate; it replicated more rapidly than HIV-1_{WT} in MT-2 cells and comparably in H9 cells. In contrast, as examined in Jurkat cells, HIV-1_{P222A} showed a substantially decreased replication rate (Fig. 5*C*). In PHA-PBM, HIV-1_{P222A} was virtually replication-incompetent (Fig. 5*D*). As expected, with the H219Q substitution added, HIV-$1_{H219Q/P222A}$ exhibited an improved replication rate, which, however, yet remained below that of HIV-1_{WT} both in Jurkat cells and PHA-PBM (Fig. 5, *C* and *D*).

These data suggested either that the added H219Q substitution enabled HIV-1_{P222A} to incorporate more CypA into daughter virions or that H219Q altered or restored a conformation of the CypA binding domain of p24 Gag protein, thereby rendering the virus replication-competent without increasing CypA content.

H219Q Substitution Improves HIV-1_{P222A} Fitness without Increasing CypA Content—In order to ask whether H219Q improved the otherwise compromised CypA incorporation caused by the P222A substitution into virions or H219Q rendered HIV-1_{P222A} replication-competent without increasing CypA content, we examined the virion-associated CypA amounts by employing Western blotting analysis.

As can be seen in Fig. 5*E-1–3*, as HIV-1 virions in the culture supernatants of chronically HIV-1-infected H9 or Jurkat cells were pelleted and subjected to Western blotting analysis for the determination of virion-associated CypA amounts using anti-p24 Gag and anti-CypA antisera, the percent densities of the CypA signal relative to each p24 Gag signal (making each p24 signal 100%) were 33.8, 8.03, 6.92, and 6.48% in Fig. 5*E-1*; 26.3, 14.1, 6.93, and 6.19% in Fig. 5*E-2*; and 16.8, 6.48, 5.72, and 5.51% in Fig. 5*E-3* for HIV-1_{WT}/H9, HIV-1_{WT}/Jurkat, HIV-1_{P222A}/H9, and HIV-$1_{H219Q/P222A}$/H9, respectively, although HIV-$1_{H219Q/P222A}$ had a greater replication rate compared with HIV-1_{P222A} (Fig. 5, *A–E*).

These data demonstrated that HIV-1_{WT} produced by Jurkat cells and HIV-1_{P222A} produced by H9 cells contained approximately less than half and approximately one-fourth of the CypA amount detected in HIV-1_{WT} produced by H9 cells, respectively. The data strongly suggested that H219Q altered the conformation of the CypA binding domain of p24 Gag protein without affecting the CypA incorporation into HIV-1_{P222A} virions, thus rendering HIV-1_{P222A} replication relatively independent of CypA. It is possible that H219Q substitution not only decreased the incorporation of CypA into HIV-1 but also altered the conformation of Gag protein, thus leading to increased HIV-1 replication especially when HIV-1 is produced in CypA-rich cells. The latter effect of H219Q substitution is apparently viable in the presence of P222A substitution because increased HIV-$1_{H219Q/P222A}$ replication was seen without significant changes in CypA content in virions (Fig. 5, *A–E*).

Molecular Modeling of the p24 Gag CA_{151}-CypA Complex with H219Q or H219P—We finally carried out molecular modeling studies to better understand the following two aspects: the reason for less viral incorporation of CypA with H219Q, H219P, and P222A substitutions, and the rescue of viral replication with the H219Q/P222A double mutation. The crystal structure determined by Gamble *et al.* (9) revealed the sequence-specific interactions of p24 Gag (CA_{151}) with CypA (Fig. 6*A*). Those interactions include seven hydrogen bonds between residues 219 and 223 (excluding the bonds mediated through bridging water molecules) and various hydrophobic contacts, all of which appear to stabilize the interactions between p24 Gag and CypA (Fig. 6*B*). Our molecular dynamics calculations for 1 ns show valuable insights to the changes in interaction between wild-type and mutated p24 Gag and CypA. Initially, the change in conformation of the wild-type structure as well as the fluctuation of the hydrogen bonds between CA and CypA at intervals of 50 ps up to 1 ns was analyzed. The backbone conformation essentially remains the same even though there is loss of the hydrogen bonds between His^{219} and $Asn^{71}{}_{CypA}$ during this dynamics calculation. The

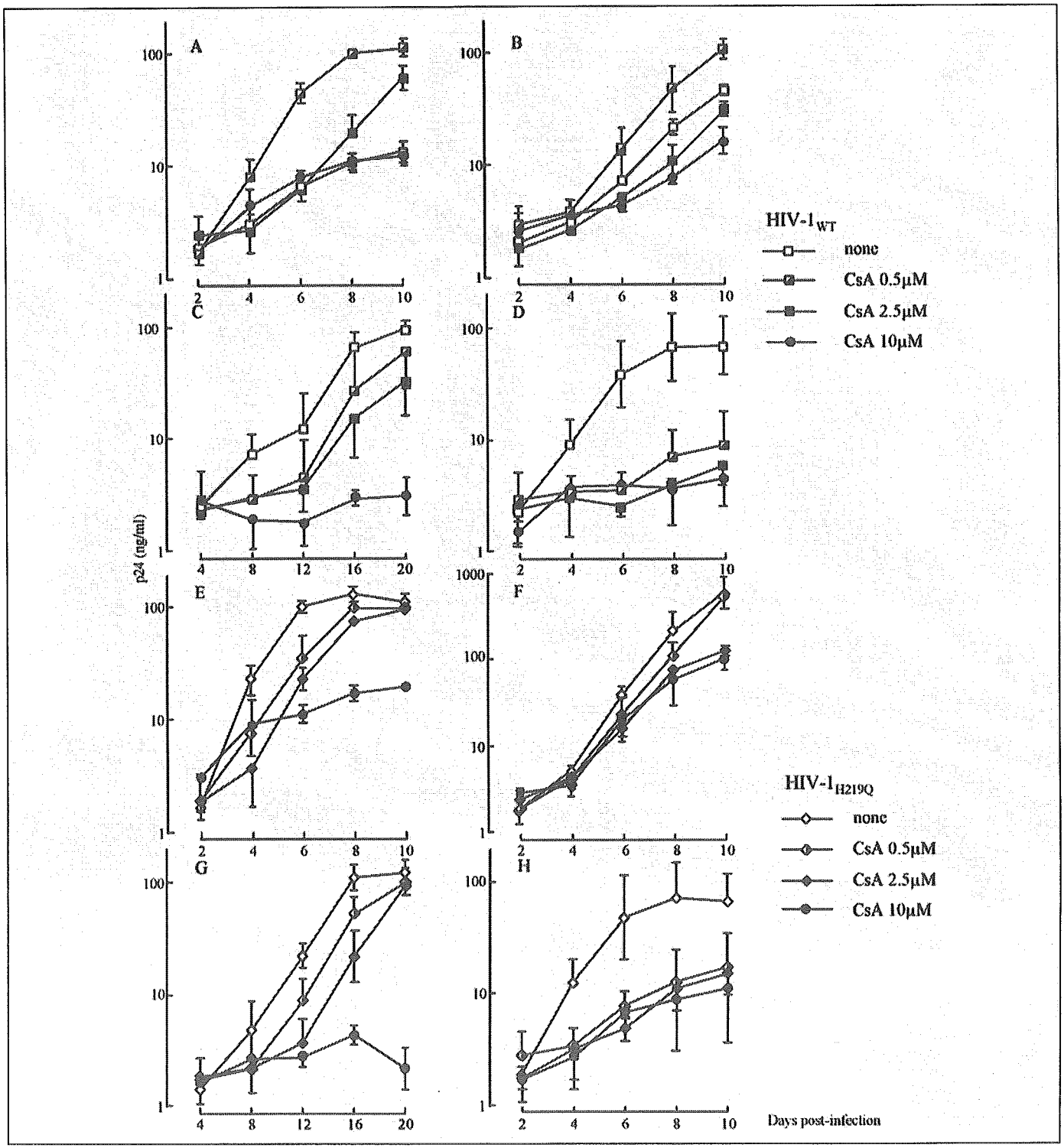

FIGURE 4. **Effects of CsA on HIV-1_{WT} and HIV-1_{H219Q} replication in various cell cultures.** MT-2 cells, H9 cells, Jurkat cells, and PHA-PBMs (*A–D*, respectively) were exposed to HIV-1_{WT} and cultured in the presence or absence of 0.5, 2.5, or 10 μM CsA. MT-2 cells, H9 cells, Jurkat cells, and PHA-PBMs (*E–H*, respectively) were also exposed to HIV-1_{H219Q} and cultured in the presence or absence of 0.5, 2.5, or 10 μM CsA. Virus replication was monitored with the amounts of p24 produced in the culture supernatants. The data shown represent geometric means (± 1 S.D.) of three independent experiments.

hydrogen bonds between Pro^{222} and $Arg^{55}{}_{CypA}$, Gly^{221}–$Asn^{102}{}_{CypA}$, and Ala^{220}–$Gln^{63}{}_{CypA}$ are the most invariant. Theses data suggest that the backbone conformation of the CypA binding region of p24 Gag is maintained with the mutation at position 219. For the mutated structures, the loop conformations at the end of 1 ns of molecular dynamics calculation were compared with the wild-type crystal structure. The weighted root mean square differences of the structures were calculated after a best fit of residues from Val^{218} to Ala^{224}. The root mean square differences of CA_{H219Q} from the wild-type CA_{151} was only 0.99 Å. Even though there is loss of hydrogen bond interactions with H219Q substitution, the loop conformations that depend on the overall conformational contact between CA and CypA do not undergo significant change (Fig. 6, *C* and *D*). The loss of the hydrogen bond between residue 219 of CA and CypA reduces the strong interaction between CA and CypA

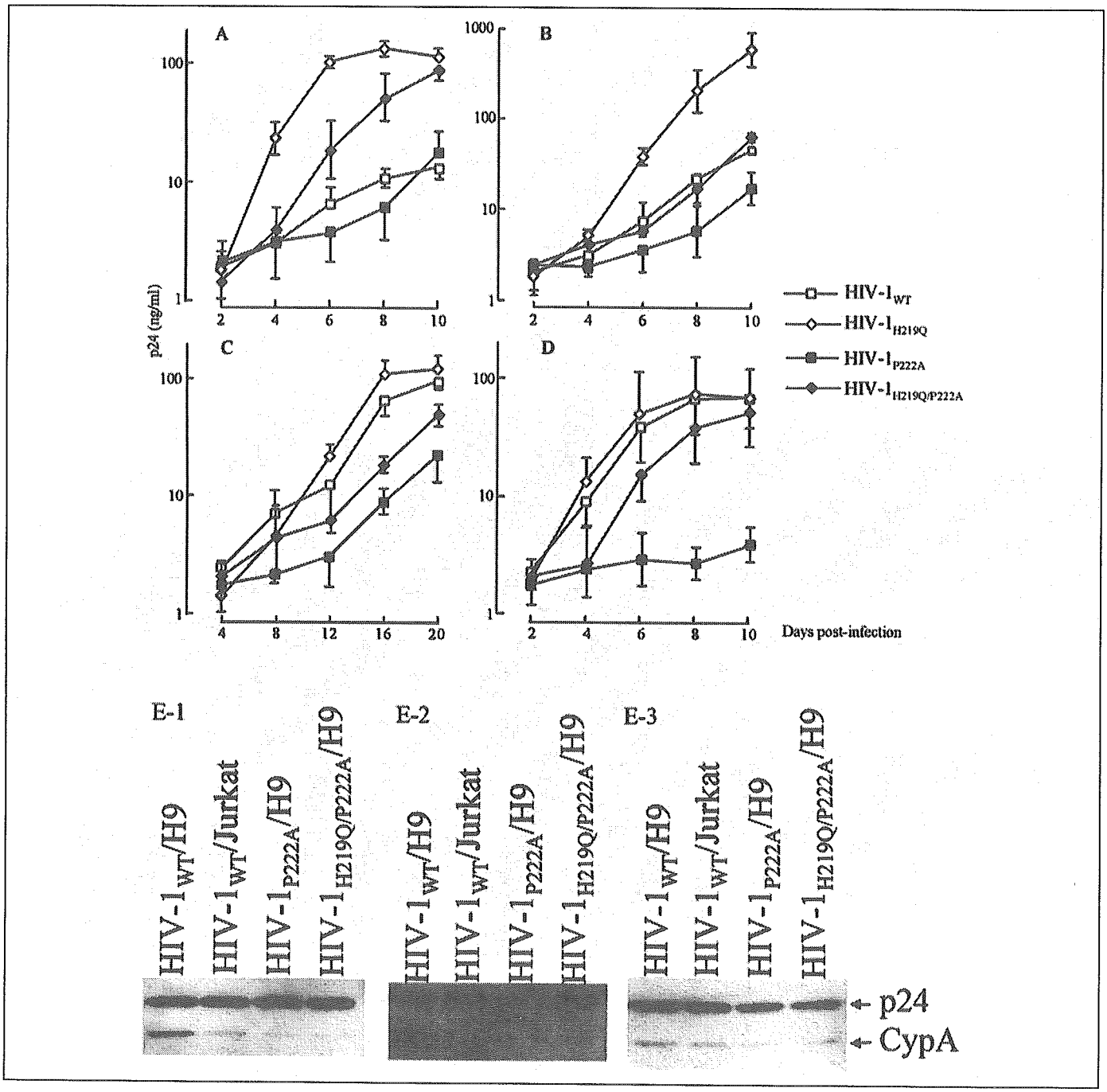

FIGURE 5. **Replication kinetics of HIV-1_{WT}, HIV-1_{H219Q}, HIV-1_{P222A}, and HIV-$1_{H219Q/P222A}$ and virion-associated CypA amounts in various HIV-1 preparations.** MT-2 cells, H9 cells, Jurkat cells, and PHA-PBMs (*A–D*, respectively) were exposed to each HIV-1 clone and cultured. Virus replication was monitored with the amount of p24 produced in the culture supernatants. The data shown represent geometric means (± 1 S.D.) of three independent experiments. HIV-1 virions in the culture supernatants of chronically HIV-1-infected H9 or Jurkat cells were pelleted and subjected to Western blotting analysis for the determination of virion-associated CypA amounts using anti-p24 Gag and anti-CypA antisera. This experiment was performed three times (*E-1–3*). Percent densities of the CypA signal relative to each p24 Gag signal (making each p24 signal 100%) were 33.8, 8.03, 6.92, and 6.48% in *E-1*; 26.3, 14.1, 6.93, and 6.19% in *E-2*; and 16.8, 6.48, 5.72, and 5.51% in *E-3* for HIV-1_{WT}/H9, HIV-1_{WT}/Jurkat, HIV-1_{P222A}/H9, and HIV-$1_{H219Q/P222A}$/H9, respectively.

and in a CypA-rich environment helps in improving viral replication. As shown in Fig. 7*A*, in the ribbon diagram of CA_{P222A} superimposed on that of CA_{WT}, CA_{P222A} causes a significant distortion of the loop structure. The value of weighted root mean square deviation of the structure of CA_{P222A} from CA_{WT} structure is 3.16 Å. In comparison, as can be seen in the ribbon diagrams of the structures of the CypA binding region of various mutant CA species (Fig. 7*B*), generated with 1-ns dynamics calculations and superimposed on the structure of CA_{WT}, H219Q and H219P substitutions do not significantly affect the conformation of the CypA binding region of CA_{WT}.

Effects of H219Q and P222A Substitutions on the Conformation of the CypA Binding Loop—It is of note that P222A not only results in less CypA incorporation but the significant change in loop conformation is probably responsible for reduction in viral replication. That the loop conformation is responsible for viral fitness is further evidenced by analysis of the structures with concurrent H219Q and P222A substitutions. These two concurrent substitutions recovered the distortion of the loop conformation that was associated with P222A mutation alone (Fig. 7*A*). Fig. 7*B* illustrates that the conformations of the CypA binding region of CA_{WT} and mutant CA species structurally resemble each other. The

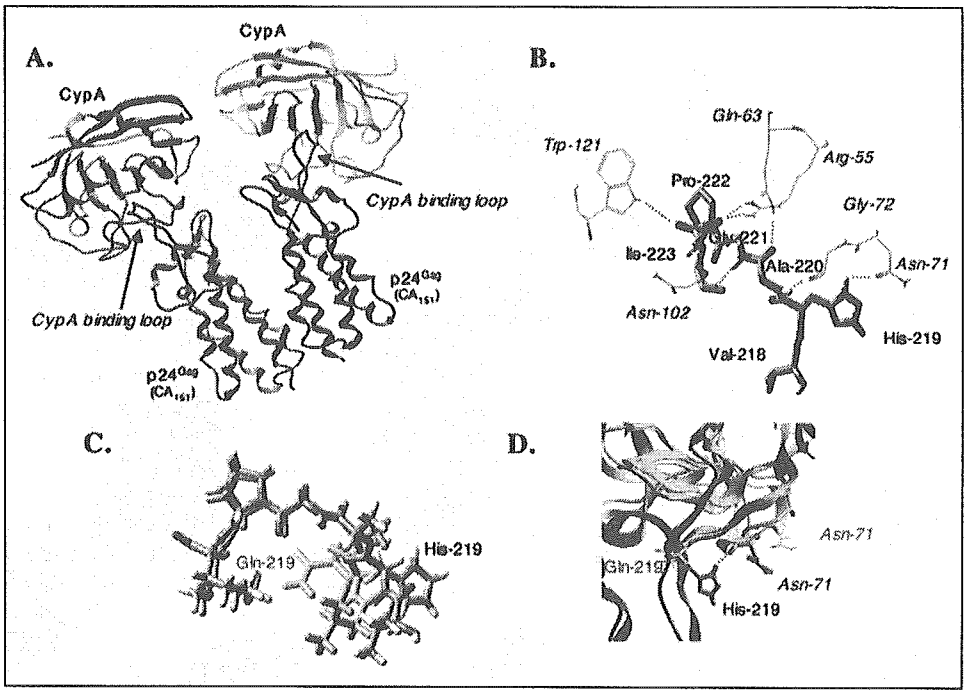

FIGURE 6. **Loss of hydrogen bonds in CA_{151}-CypA complex with H219Q or H219P substitution.** *A*, there are two p24 Gag CA_{151}-CypA complexes in the asymmetric unit (9). *B*, in the area of the CypA binding loop shown there are seven hydrogen bonds, which are between His^{219}–$Asn^{71}{}_{CypA}$, Ala^{220}–$Gln^{63}{}_{CypA}$, Ala^{220}–$Gly^{72}{}_{CypA}$, Gly^{221}–$Asn^{102}{}_{CypA}$, Pro^{222}–$Arg^{55}{}_{CypA}$ (two hydrogen bonds), and Ile^{223}–$Trp^{121}{}_{CypA}$. These hydrogen bonds along with hydrophobic contacts are responsible for maintaining the optimum relative conformations of p24 and CypA. *C*, H219Q substitution results in the loss of the following three hydrogen bond interactions: Gln^{219}–$Asn^{71}{}_{CypA}$, Ala^{220}–$Gly^{72}{}_{CypA}$, and Ile^{223}–$Trp^{121}{}_{CypA}$ and causes a significant conformational change of the contact region of the CypA binding loop (see *D*). *D*, changes in the complex configurations with H219Q substitution. Note that in the mutated structure Gln^{219} (*wire*) is located far apart from $Asn^{71}{}_{CypA}$ (*wire*), although in the wild-type structure His^{219} (*stick*) forms a tight hydrogen bond with $Asn^{71}{}_{CypA}$ (*stick*). CA_{WT} is shown by a *green ribbon* and the complexed CypA by a *yellow ribbon*; CA_{H219Q} is shown by a *red tube* and the complexed CypA by a *pink tube*. The loss of hydrogen bonds results in reduced CypA incorporation, but there persists sufficient interaction so that there are minimal alterations in the conformation of the CypA binding loop of CA_{151}.

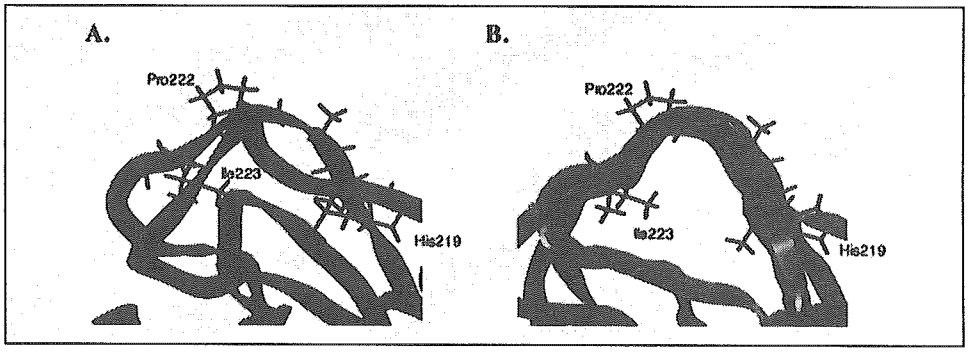

FIGURE 7. **Loop conformations of CA_{WT} and CA_{MT}.** *A*, ribbon diagram of CA_{P222A} (*purple*) superimposed on that of CA_{WT} (*red*). CA_{P222A} causes a significant distortion of the loop structure. The value of weighted root mean square deviation of the structure of CA_{P222A} from CA_{WT} structure is 3.16 Å. *B*, ribbon diagrams of the structures of the CypA binding region of various CA_{MT}, generated with 1-ns dynamics calculations, are superimposed on the structure of CA_{WT}. CA_{WT} is shown in *red*, CA_{H219Q} in *yellow*, CA_{H219P} in *blue*, $CA_{H219Q/P222A}$ in *magenta*, and $CA_{P222A/A224E}$ in *cyan*. *Residues 218–223 of* CA_{WT} are shown as *red sticks*. The values of weighted root mean square deviation of CA_{H219Q}, CA_{H219P}, $CA_{H219Q/P222A}$, and $CA_{P222A/A224E}$ structures from CA_{WT} structure are 0.99, 1.77, 1.24, and 1.48 Å, respectively. H219Q and H219P substitutions do not significantly affect the conformation of the CypA binding region of CA_{WT}. Note that the conformations of the CypA binding region of CA_{WT} and mutant CA species structurally resemble each other. Also note that $CA_{H219Q/P222A}$ and $CA_{P222A/A224E}$ have the conformation of the CypA binding loop region restored close to that of CA_{WT} in comparison with CA_{P222A}.

values of weighted root mean square deviation of CA_{H219Q}, CA_{H219P}, and $CA_{H219Q/P222A}$ structures from CA_{WT} structure were 0.99, 1.77, and 1.24 Å, respectively. Thus, it was thought that the restoration of the distorted conformation of the CypA binding loop caused by H219Q and P222A substitutions were presumably responsible for the improved replication compared with HIV-1_{P222A}, particularly in PHA-PBM where CypA contents are significantly less in comparison with MT-2 and H9 cells (Fig. 3 and Fig. 5, *A–D*).

As noted above, when HIV-1_{NL4-3} was propagated in the absence of PI in MT-2 cells, the virus also acquired A224V mutation by passage 10 (4). It should be noted that Ala^{224} is also located within the CypA binding loop of p24 Gag protein and is also known to interact with CypA through hydrophobic contacts (9). Therefore, we also examined the highly intriguing findings by Braaten and co-workers (24) that the addition of A224E substitution rescued the replication of an otherwise poorly replicating HIV-1_{P222A} without increasing the level of viral CypA incorporation that had been reduced by P222A substitution. As shown in Fig. 7*B*, the loop conformation, with the two amino acid substitutions, is restored closely to that of the wild-type conformation. The values of weighted root mean square deviation of $CA_{P222A/A224E}$ structure from CA_{WT} structure was 1.48 Å. This observation should corroborate our observation that the conformation of the CypA binding region of capsid is critical for viral fitness.

DISCUSSION

It should be noted that certain polymorphic amino acid residues seen in HIV-1 strains are associated with HIV-1 drug resistance (2, 3). It is also known that certain drug resistance-conferring amino acid substitutions found in one subtype HIV-1 isolated from patients under therapy may be detected in HIV-1 of other subtypes from individuals having received no therapy (25, 26). Moreover, a recent study by Colson *et al.* (27) has revealed that HIV-2 strains harbor specific patterns of natural polymorphism and resistance. It is particularly of note that out of 88 different HIV-1 strains compiled in the HIV Sequence Compendium 2000 (22), 65 had histidine at position 219, whereas13 had glutamine, and 4 had proline. Hence, as studied in this work both Gln^{219} and Pro^{219} represent polymorphic amino acid residues, and it is thought that these

two polymorphic amino acids are associated with the acquisition of resistance to certain PIs.

In the present study, we found that the two substitutions H219Q and H219P were closely associated with replication advantages when propagated in CypA-rich MT-2 and H9 cells. The same advantage was seen in PHA-PBM containing a smaller amount of CypA, but only in a limited fashion (Fig. 2 and Fig. 3, *A* and *B*). We also found that these substitutions reduced CypA incorporation into virions (Fig. 3*C*), which is compatible with previous reports by two groups (28, 29). It was therefore postulated that MT-2 and H9 cells contained high CypA amounts, thereby compromising HIV-1_{WT} replication. However, H219Q and H219P substitutions apparently reduced the viral interaction with CypA, resulting in enhanced HIV-1 replication (Figs. 2 and 3). Most interestingly, when HIV-1_{H219Q} was exposed to CsA (0.5 μM), its replication was suppressed, unlike that of HIV-1_{WT}, and the higher CsA concentration (2.5 μM) further suppressed HIV-1_{H219Q} replication in all the cell preparations examined (Fig. 4). It is noteworthy that Braaten *et al.* (5) reported that virion-associated CypA amounts were reduced by 50 and 75% when HIV-1 was propagated in the presence of 0.5 and 2.5 μM CsA, respectively. Although the exact role of CypA in HIV-1 replication is as yet unclear, CypA seems to play a critical role early in the HIV-1 replication cycle (5, 8, 30) by destabilizing the capsid (p24)-capsid interactions, thereby promoting disassembly of the viral core (9). An excessive depletion of CypA may tighten capsid-capsid binding, thereby interfering with virion uncoating and reducing HIV-1 replication rates, although such a sequel is speculative at present. On the other hand, higher amounts of CypA may greatly destabilize capsid-capsid interactions, thereby rendering the virion core unstable and likewise decrease HIV-1 replication (23). Thus, it was thought that the CsA-induced HIV-1_{H219Q} replication reduction in MT-2 and H9 cells was because of an excessive depletion of CypA. It is also of note that our observation that CsA potentiated HIV-1_{WT} replication in MT-2 and H9 cells, although it failed to boost HIV-1_{H219Q} replication, makes our view more plausible that H219Q substitution is directly responsible for the increased viral replication and the reduction of CypA content in daughter virions.

The presence of Pro at position 222 in p24 Gag protein has been shown to be a primary determinant of CypA binding (9), and its substitution to Ala (P222A) decreases viral CypA incorporation, causing reduced HIV-1 replication in Jurkat cells (5, 6). In this regard, HIV-1_{P222A} was originally reported to have a severely compromised infectivity in Jurkat cells (5, 6), but it was later reported that CypA-rich H9 and CEM cells could support the replication of HIV-1_{P222A} (23, 31). In the present study, we also found that the P222A substitution reduced CypA incorporation by HIV-1 by ~75% (Fig. 5*E*) and significantly reduced HIV-1 replication in Jurkat cells and PHA-PBM, which contained relatively low CypA amounts (Fig. 3, *A* and *B*). We presumed that the introduction of H219Q substitution, which decreases p24 Gag protein binding to CypA (Fig. 3*C*), to HIV-1_{P222A} would further decrease viral CypA incorporation and thereby replication. It was intriguing that the H219Q substitution added to HIV-1_{P222A} potentiated HIV-1 replication as examined in all the cell preparations used (Fig. 5, *A–D*). These data suggest either that the added H219Q substitution enabled HIV-1_{P222A} to incorporate more CypA into daughter virions or altered a conformation of the CypA binding domain of p24 Gag protein, thereby rendering the virus relatively independent of CypA. In fact, the virus-associated CypA amount in HIV-$1_{H219Q/P222A}$ was less than or comparable with that in HIV-1_{P222A} (Fig. 5*E*). It is worth noting that a substitution at position 224 of p24 Gag protein from Ala to Glu (A224E) recovers the compromised replication of HIV-1_{P222A} in Jurkat cells but does not alter the viral CypA incorporation (24). It is also worth noting that even though all the amino acid substitutions examined here decreased viral CypA incorporation, only P222A substitution decreased viral replication. We showed that the loop conformation of the CypA binding region of CA_{WT}, CA_{H219Q}, and CA_{H219P} was quite similar to each other, whereas the conformation of CA_{P222A} sustained the most distortion (Fig. 7, *A* and *B*). It should be noted that $CA_{H219Q/P222A}$ and $CA_{P222A/A224E}$ (24) not only improve viral replication over CA_{P222A} but also restored their conformation (Fig. 5, *A–D*, and Fig. 7, *A* and *B*). We postulate that the conformation of the CypA binding region of CA_{151} is strongly correlated with viral fitness, and the functional role of CypA is to maintain the conformation of CA_{151} for viral replication.

It should be noted that HIV-1 infection of simian cells is restricted at an early post-entry step by the presence of simian TRIM5α (tripartite motif 5α) (32). In this respect, replacement of HIV-1 capsid protein with simian immunodeficiency virus capsid sequence significantly reduced the simian TRIM5α-mediated restrictions, demonstrating that the capsid protein of HIV-1 is a critical viral determinant for susceptibility to post-entry restriction in simian cells (33). Most interestingly, H219Q substitution of HIV-1 capsid is reported to be associated with the reduction of simian TRIM5α-mediated restriction (34, 35), suggesting that conformational change of CypA binding loop by H219Q, as we described in this work, might reduce the recognition by simian TRIM5α. It is also possible that the effects of H219Q observed in this study involve alterations of the interaction of TRIM5α and/or TRIM5α cofactors with the HIV-1 capsid. It is noteworthy that human TRIM5α, which has been shown to partly restrict HIV-1 infection (32), may be contributing to the effects on HIV-1 replication that occur when CypA is not able to bind the capsid protein of HIV-1 (36).

In summary, our study suggests that the H219Q substitution increases HIV-1 replication through (i) maintaining the loop conformation of CypA binding region and (ii) providing favorable conditions for viral replication by reducing viral CypA incorporation. The present data also show that the replication of HIV-1 with $CA_{H219Q/P222A}$ and that with $CA_{P222A/A224E}$, as studied elsewhere (24), were restored as compared with the otherwise compromised replication of HIV-1 with CA_{P222A} by restoring the loop conformation without increasing CypA content. We believe that an optimal concentration of CypA, which is neither excessively high nor excessively low, is critical for viral fitness and that the functional role of CypA is to maintain the conformation of CA_{151}.

Acknowledgments—We are grateful to Douglas Braaten and Jeremy Luban for kindly providing the plasmid of HIV-1_{P222A}; Mark K. Kavlick for technical assistance and helpful discussion; and the Center for Information Technology, National Institutes of Health, for computational resources.

REFERENCES

1. Mitsuya, H., and Erickson, J. (1999) in *Textbook of AIDS Medicine* (Merigan, T. C., Bartlet, J. G., and Bolognesi, D., eds) pp. 751–780, Williams & Wilkins, Baltimore
2. Kavlick, M. F., and Mitsuya, H. (2001) in *Art of Antiretroviral Therapy* (De Clarcq, R., ed) pp. 279–312, American Society for Microbiology, Washington, D. C.
3. Tanaka, M., Srinivas, R. V., Ueno, T., Kavlick, M. F., Hui, F. K., Fridland, A., Driscoll, J. S., and Mitsuya, H. (1997) *Antimicrob. Agents Chemother.* **41**, 1313–1318
4. Gatanaga, H., Suzuki, Y., Tsang, H., Yoshimura, K., Kavlick, M. F., Nagashima, K., Gorelick, R. J., Mardy, S., Tang, C., Summers, M. F., and Mitsuya, H. (2002) *J. Biol. Chem.* **277**, 5952–5961
5. Braaten, D., Franke, E. K., and Luban, J. (1996) *J. Virol.* **70**, 3551–3560
6. Franke, E. K., Yuan, H. E., and Luban, J. (1994) *Nature* **372**, 359–362
7. Braaten, D., and Luban, J. (2001) *EMBO J.* **20**, 1300–1309
8. Steinkasserer, A., Harrison, R., Billich, A., Hammerschmid, F., Werner, G., Wolff, B., Peichl, P., Palfi, G., Schnitzel, W., Mlynar, E., and Rosenwirth, B. (1995) *J. Virol.* **69**, 814–824
9. Gamble, T. R., Vajdos, F. F., Yoo, S., Worthylake, D. K., Houseweart, M., Sundquist,